Phenomenological analysis of charmless decays $B_s \to PP, PV$ with QCD factorization

Junfeng Sun*
Institute of High Energy Physics, Chinese Academy of Sciences, P.O. Box 918(4), Beijing 100039, China

Guohuai Zhu†
Theory Group, KEK, Tsukuba, Ibaraki 305-0801, Japan

Dongsheng Du‡
Institute of High Energy Physics, Chinese Academy of Sciences, P.O. Box 918(4), Beijing 100039, China
(Received 11 November 2002; revised manuscript received 3 March 2003; published 3 September 2003)

We calculate the *CP*-averaged branching ratios and *CP*-violating asymmetries of two-body charmless hadronic decays of $B_s \to PP, PV$ with the QCD factorization approach (here P and V denote pseudoscalar and vector mesons, respectively), including contributions from the chirally enhanced power corrections and weak annihilations. Only several decay modes, such as $B_s \to K^{(*)}K$, $K^{(*)\pm}\pi^{\mp}$, $K^{\pm}\rho^{\mp}$, $\eta^{(\prime)}\eta^{(\prime)}$, have large branching ratios, which may be observed in the near future. We also discuss $B_s \to K^+K^-$, $K^0\overline{K}^0$ decays which could overconstrain the penguin-to-tree ratio $|P_{\pi\pi}/T_{\pi\pi}|$ of $B \to \pi^+\pi^-$ decays and give a bound on the Cabibbo-Kobayashi-Maskawa angle γ.

DOI: 10.1103/PhysRevD.68.054003 PACS number(s): 13.25.Hw, 12.38.Bx

I. INTRODUCTION

Recently there has been remarkable progress in the study of exclusive charmless $B_{u,d}$ decays. Experimentally, many two-body nonleptonic charmless $B_{u,d}$ decays have been observed by CLEO and B factories at KEK and SLAC (see Refs. [1–10]), and more B decay channels will be measured with great precision soon. Theoretically, several attractive methods have been proposed to study the nonfactorizable effects in hadronic matrix elements from first principles, such as QCD factorization (QCDF) [11], the perturbative QCD method (PQCD) [12–14], and so on. Intensive investigations of hadronic charmless two-body $B_{u,d}$ decays have been studied in detail, for example, in Refs. [15–22].

The potential B_s decay modes allow us to overconstrain the angles and sides of the *unitarity triangle* [the unitarity relation between the first and the third column of the Cabibbo-Kobayashi-Maskawa (CKM) matrix [23] of weak interactions]. This makes the search for *CP* violation in the B_s decays highly interesting. The problem is that B_s mesons oscillate at a high frequency and nonleptonic B_s decays still remain elusive from observation. At present, only some weak upper limits on branching ratios of several charmless hadronic decays are available, mostly from CERN e^+e^- collider LEP and SLAC Large Detector (SLD) experiments [24], such as $B_s^0 \to \pi^+\pi^-, \pi^0\pi^0, \eta\pi^0, \eta\eta, K^+K^-, \pi^+K^-, \ldots$. Unlike $B_{u,d}$ mesons, the heavier B_s mesons cannot be studied at B factories operating at the $\Upsilon(4S)$ resonance. However, it is believed that in the future at hadron colliders, such as the Collider Detector at Fermilab (CDF), D0, DESY *ep* collider HERA-B, BTeV, and CERN Large Hadron Collider (LHCb), the signs of *CP* violation in B_s system can be observed with high accuracy in addition to studies of certain $B_{u,d}$ modes.

Early theoretical studies of charmless nonleptonic B_s decays can be found in Refs. [25–29]. The investigation of the exclusive charmless B_s decays into final states containing an $\eta^{(\prime)}$ meson was given within the generalized factorization framework [30]. Chen, Cheng, and Tseng calculated carefully the branching ratios for the charmless decays $B_s \to PP, PV, VV$ (here P and V denote pseudoscalar and vector mesons, respectively) [31]. And new physics effects in B_s decays were considered in [32]. It is found that the electroweak penguin contributions can be large for some decays modes [29,31] and that branching ratios for $B_s \to \eta\eta'$ and several other decay modes can be as large as 10^{-5} [30–32] which is measurable at future experiments.

A few years ago, Beneke *et al.* suggested a QCDF formula to compute the hadronic matrix elements $\langle M_1 M_2|O_i|B\rangle$ in the heavy quark limit, combining the hard scattering approach with power counting in $1/m_b$ [11] (where m_b is the mass of b quark). At leading order of the heavy quark expansion, the hadronic matrix elements can be factorized into perturbatively calculable hard scattering kernels and a universal nonperturbative part parametrized by the form factors and meson light cone distribution amplitudes. This basic formula is valid for B decays into two light final states [11,33]. We made a comprehensive analysis of exclusive hadronic $B_{u,d}$ decays using the QCDF approach to estimate the *CP*-averaged branching ratios and *CP*-violating asymmetries for decays $B_{u,d} \to PP$ [21] and PV [22] and found that, with appropriate parameters, most of the QCDF predictions were in agreement with the present experimental data. In Ref. [34] we do a global analysis of $B_{u,d} \to PP, PV$ decays by comparing measurements with their corresponding theoretical results and find that the QCDF approach is a promising method for dealing with charmless two-body $B_{u,d}$

*Email address: sunjf@mail.ihep.ac.cn
†Email address: zhugh@post.kek.jp.
‡Email address: duds@mail.ihep.ac.cn

 ©2003 The American Physical Society

TABLE I. Wilson coefficients $C_i(\mu)$ in the naive dimensional regularization (NDR) scheme for $\alpha_s(m_Z)=0.117$, $\alpha_{em}(m_W)=1/128$, $m_W=80.42$ GeV, $m_Z=91.188$ GeV, $m_t=178.1$ GeV, and $m_b=4.66$ GeV.

	$\mu=m_b/2$		$\mu=m_b$		$\mu=2m_b$	
	NLO	LO	NLO	LO	NLO	LO
C_1	1.130	1.171	1.078	1.111	1.042	1.071
C_2	−0.274	−0.342	−0.176	−0.238	−0.102	−0.161
C_3	0.021	0.019	0.014	0.012	0.009	0.007
C_4	−0.048	−0.047	−0.034	−0.032	−0.024	−0.022
C_5	0.010	0.010	0.008	0.008	0.007	0.006
C_6	−0.060	−0.058	−0.039	−0.037	−0.026	−0.023
C_7/α_{em}	−0.005	−0.105	0.011	−0.097	0.035	−0.081
C_8/α_{em}	0.086	0.023	0.055	0.014	0.036	0.009
C_9/α_{em}	−1.419	−0.091	−1.341	−0.087	−1.277	−0.075
C_{10}/α_{em}	0.383	−0.021	0.264	−0.016	0.176	−0.011
$C_{7\gamma}$		−0.342		−0.306		−0.276
C_{8g}		−0.160		−0.146		−0.133

decays. In this paper, we would like to apply the QCDF approach to the case of B_s mesons.

This paper is organized as follows. In Sec. II, we discuss the theoretical framework and define the relevant matrix elements for $B_s\to PP,PV$ decays. In Sec. III, we list the theoretical input parameters used in our analysis. Sections IV and V are devoted to numerical results and some remarks on *CP*-averaged branching ratios and *CP*-violating asymmetries, respectively. In addition, theoretical uncertainties due to variation of the inputs are investigated. In Sec. VI, we discuss $B_s\to K^+K^-,K^0\bar{K}^0$ decays which could overconstrain the penguin-to-tree ratio $P_{\pi\pi}/T_{\pi\pi}$ of $B\to\pi^+\pi^-$ decays and the CKM angle γ. Finally, we conclude with a summary in Sec. VII.

II. THEORETICAL FRAMEWORK FOR *B* DECAYS

A. Effective Hamiltonian

Using the operator product expansion and renormalization group equation, the low energy effective Hamiltonian relevant to nonleptonic B decays can be written as [35]

$$\mathcal{H}_{eff}=\frac{G_F}{\sqrt{2}}\sum_{q=u,c} v_q\Bigg\{C_1(\mu)Q_1^q(\mu)+C_2(\mu)Q_2^q(\mu)+\sum_{k=3}^{10} C_k(\mu)Q_k(\mu)+C_{7\gamma}Q_{7\gamma}+C_{8g}Q_{8g}\Bigg\}+\text{H.c.}, \tag{1}$$

where $v_q=V_{qb}V_{qd}^*$ (for $b\to d$ transition) or $v_q=V_{qb}V_{qs}^*$ (for $b\to s$ transition) are CKM factors. The couplings $C_i(\mu)$ are Wilson coefficients which have been reliably evaluated to the next-to-leading logarithmic order [35]. Their numerical values in the naive dimensional regularization (NDR) scheme at three different scales are listed in Table I. The effective operators Q_i can be expressed explicitly as follows:

$$Q_1^u=(\bar{u}_\alpha b_\alpha)_{V-A}(\bar{q}_\beta u_\beta)_{V-A},\qquad Q_1^c=(\bar{c}_\alpha b_\alpha)_{V-A}(\bar{q}_\beta c_\beta)_{V-A}, \tag{2}$$

$$Q_2^u=(\bar{u}_\alpha b_\beta)_{V-A}(\bar{q}_\beta u_\alpha)_{V-A},\qquad Q_2^c=(\bar{c}_\alpha b_\beta)_{V-A}(\bar{q}_\beta c_\alpha)_{V-A}, \tag{3}$$

$$Q_3=(\bar{q}_\alpha b_\alpha)_{V-A}\sum_{q'}(\bar{q}'_\beta q'_\beta)_{V-A}, \tag{4}$$

$$Q_4=(\bar{q}_\beta b_\alpha)_{V-A}\sum_{q'}(\bar{q}'_\alpha q'_\beta)_{V-A}, \tag{5}$$

$$Q_5=(\bar{q}_\alpha b_\alpha)_{V-A}\sum_{q'}(\bar{q}'_\beta q'_\beta)_{V+A}, \tag{6}$$

$$Q_6=(\bar{q}_\beta b_\alpha)_{V-A}\sum_{q'}(\bar{q}'_\alpha q'_\beta)_{V+A}, \tag{7}$$

$$Q_7=\frac{3}{2}(\bar{q}_\alpha b_\alpha)_{V-A}\sum_{q'} e_{q'}(\bar{q}'_\beta q'_\beta)_{V+A},\qquad Q_8=\frac{3}{2}(\bar{q}_\beta b_\alpha)_{V-A}\sum_{q'} e_{q'}(\bar{q}'_\alpha q'_\beta)_{V+A},$$

$$Q_9=\frac{3}{2}(\bar{q}_\alpha b_\alpha)_{V-A}\sum_{q'} e_{q'}(\bar{q}'_\beta q'_\beta)_{V-A},\qquad Q_{10}=\frac{3}{2}(\bar{q}_\beta b_\alpha)_{V-A}\sum_{q'} e_{q'}(\bar{q}'_\alpha q'_\beta)_{V-A}, \tag{8}$$

$$Q_{7\gamma}=\frac{e}{8\pi^2}m_b\bar{q}_\alpha\sigma^{\mu\nu}(1+\gamma_5)b_\alpha F_{\mu\nu},\qquad Q_{8g}=\frac{g}{8\pi^2}m_b\bar{q}_\alpha\sigma^{\mu\nu}(1+\gamma_5)t^a_{\alpha\beta}b_\beta G^a_{\mu\nu},$$

where q' denotes all the active quarks at scale $\mu=\mathcal{O}(m_b)$: i.e., $q'=u,d,s,c,b$.

B. Hadronic matrix elements within the QCDF framework

To get the decay amplitudes, the most difficult theoretical work is to compute the hadronic matrix elements of the effective operators: i.e., $\langle M_1M_2|O_i|B\rangle$. Phenomenologically, these hadronic matrix elements are usually parametrized into the product of the decay constants and the transition form factors based on the naive factorization (NF) scheme [36]. However, one main defect of the NF approach is that hadronic matrix elements cannot make compensation for the renormalization scheme and scale dependences of Wilson coefficients; in this sense, the NF results are unphysical. This

indicates that ''nonfactorizable'' contributions to the hadronic matrix elements must be taken into account.

The QCDF approach is one of the novel methods to evaluate these hadronic matrix elements relevant to B decays systematically. In the heavy quark limit $m_b \gg \Lambda_{QCD}$, to leading power corrections in Λ_{QCD}/m_b, the basic QCDF formula is given by [11]

$$\begin{aligned}\langle M_1 M_2|O_i|B\rangle &= \sum_j F_j^{B\to M_1}\int_0^1 dx T_{ij}^I(x)\Phi_{M_2}(x)\\ &\quad +(M_1\leftrightarrow M_2)\\ &\quad +\int_0^1 d\xi\int_0^1 dx\int_0^1 dy T_i^{II}(\xi,x,y)\\ &\quad \times\Phi_B(\xi)\Phi_{M_1}(x)\Phi_{M_2}(y)\\ &= \langle M_1 M_2|J_1\otimes J_2|B\rangle_F\Big[1+\sum r_n\alpha_s^n\\ &\quad +\mathcal{O}(\Lambda_{QCD}/m_b)\Big],\end{aligned} \tag{9}$$

where $T_i^{I,II}$ denote hard scattering kernels. At leading order of α_s, $T_i^I=1$, $T_i^{II}=0$, the QCDF formula (9) shows that there is no long-distance interaction between the M_2 meson and (BM_1) systems (where M_1 denotes the meson that picks up the spectator quark in the B meson) and reproduces the NF results. Neglecting the power corrections of $\mathcal{O}(\Lambda_{QCD}/m_b)$, $T_i^{I,II}$ are hard gluon exchange dominant and, therefore, calculable order by order with perturbation theory. Nonperturbative effects are either suppressed by $1/m_b$ or parametrized in terms of mesons decay constants, form factors $F^{B\to M_1}$, and meson light cone distribution amplitudes $\Phi_B(\xi),\Phi_M(x)$. The factorized matrix elements $\langle M_1M_2|J_1\otimes J_2|B\rangle_F$ are the same as the definition of the Bauer-Stech-Wirbel (BSW) approximation [36]. Through the QCDF formula, the hadronic matrix elements can be separated into a short-distance part and a long-distance part, and the renormalization scheme and scale dependences of the hadronic matrix elements can cancel those of the corresponding Wilson coefficients, so that physical results are—at least at the order of α_s—renormalization scheme and scale independent [33]. Through the QCDF formula, ''nonfactorizable'' effects can be evaluated, and partial information about the final states interactions and the strong phases can be obtained.

It is important to note that some power suppression might fail in some cases because the b quark mass is not asymptotically large. For example, the power correction proportional to $2m_M^2/(m_b m_q)$ with $q=u,d,s$, which is formally power suppressed, is now chirally enhanced and numerically important to penguin-dominated B rare decays. Therefore it is necessary to include at least the chirally enhanced corrections consistently for phenomenological application of the QCDF approach in B decays. However, it is shown in [20,33] that for $B\to PP$ decays, the contributions of twist-3 light cone distribution amplitudes to hard scattering kernels cannot provide sufficient end-point suppression when the spectator quark in the B meson enters the final-state meson as a soft quark, so there appears infrared logarithmic divergence $\int dx/x\sim\ln(m_b/\Lambda_{QCD})$. But there is no such problem within the PQCD approach by introducing the partonic intrinsic transverse momentum and the mechanism of Sudakov suppression to regulate the end-point singularities. So it is interesting to investigate the possibility of incorporating Sudakov form factor into the QCDF approach, such as [37]. But it is controversial to invoke Sudakov effects for hadronic B decays. For example, Descotes-Genon and Sachrajda studied Sudakov effects in the form factors $F^{B\to\pi}$ of $B\to\pi l\nu_l$ decays and claimed that the PQCD approach also could not make reliable predictions for such a kind of process [38]. Likewise, Wei and Yang's analysis [39] indicated that Sudakov suppression is not efficient enough, and the validity of the PQCD approach for B decays is questionable. Here we will bypass this problem and adopt the conventions in [20], treating the logarithmically divergent integrals phenomenologically [see Eq. (28)].

For weak annihilation contributions, they are believed to be very small with the naive factorization assumption (see, for example, Ref. [15]). Within the QCDF approach, the weak annihilation amplitudes are formally suppressed by $(f_B f_{M_1})/(F^{B\to M_1}m_B^2)\sim\Lambda_{QCD}/m_b$ with the power counting ansatz of Ref. [11]. But as emphasized in [14,40,41], annihilation contributions with QCD corrections could give potentially large strong phases; hence, large CP violation could be expected. In addition, phenomenological investigations of B decays [20–22] within the QCDF framework also suggest that their effects could be sizable when large model uncertainties are considered. So annihilation contributions cannot be simply neglected. In this paper, we follow the treatments in [20] to estimate the annihilation effects, including the contributions of chirally enhanced twist-3 light cone distribution amplitudes. It is also interesting to notice that [20–22] weak annihilation contributions exhibit end-point singularities even at leading twist order of light cone distribution amplitudes for the final states. Similar to the case of twist-3 hard spectator scattering kernels, these infrared divergence can be parametrized phenomenologically, with the price of introducing extra theoretical uncertainties and model dependence.

In summary, the hadronic matrix elements for two-body B_s decays can be written as

$$\langle M_1M_2|\mathcal{H}_{eff}|B_s\rangle = \mathcal{A}^f(B_s\to M_1M_2)+\mathcal{A}^a(B_s\to M_1M_2), \tag{10}$$

$$\begin{aligned}\mathcal{A}^f(B_s\to M_1M_2) &= \frac{G_F}{\sqrt{2}}\sum_{q=u,c}\sum_{i=1}^{10} v_q a_i^q\\ &\quad\times\langle M_1M_2|J_1\otimes J_2|B_s\rangle_F,\end{aligned} \tag{11}$$

$$\mathcal{A}^a(B_s\to M_1M_2)\propto\frac{G_F}{\sqrt{2}}\sum_{q=u,c}\sum_i f_{B_s}f_{M_1}f_{M_2}v_q b_i, \tag{12}$$

where $\mathcal{A}^a$ represents weak annihilation contributions. f_{B_s} and f_M are decay constants for B_s, and M mesons, respec-

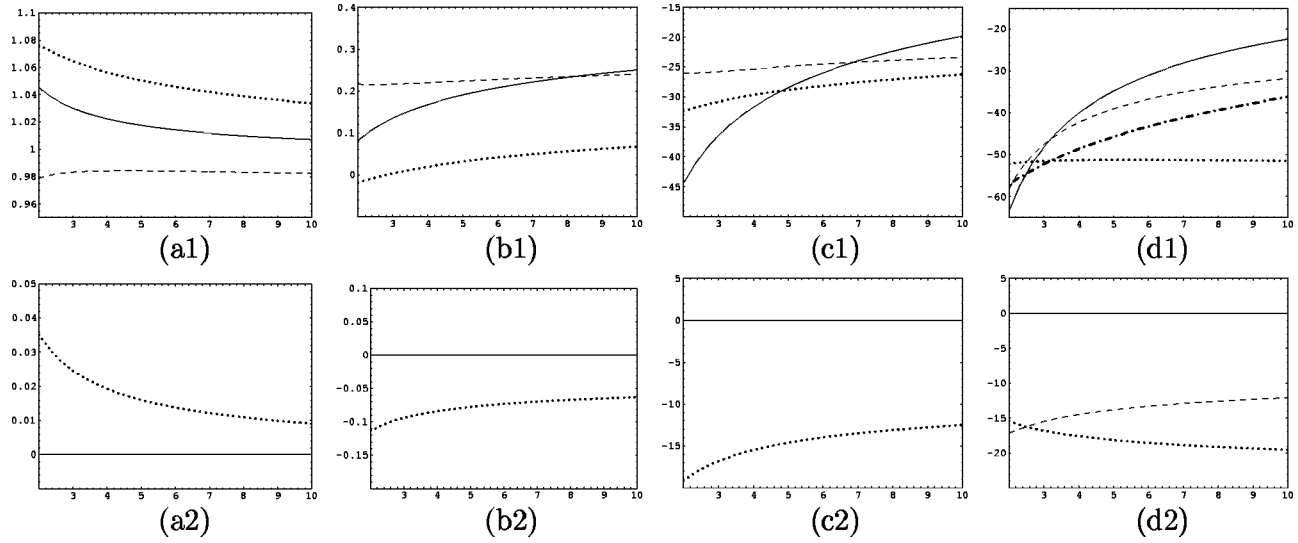

FIG. 1. Dependence of the coefficients $a_i(KK)$ (vertical axes) on the renormalization scale μ (horizontal axes, in units of GeV), with asymptotic meson light cone distribution amplitudes and the default values of inputs. In (a1), the solid line denotes $\mathrm{Re}(a_1^u)$ within the NF framework; the dotted and dashed lines denote $\mathrm{Re}(a_{1,I}^u)$ and $\mathrm{Re}(a_1^u)$ within the QCDF framework, respectively. In (a2), the solid and dashed lines denote $\mathrm{Im}(a_1^u)$ within the NF and QCDF framework, respectively. Coefficients a_2^u and $a_4^u\times 10^3$ versus scale μ are shown in (b) and (c), respectively. In (d), the solid and dashed lines denote $a_6^u\times 10^3$, and the legends are the same as in (a), while the dot-dashed and dotted lines show $a_6^u r_\chi\times 10^3$ within the NF and QCDF framework, respectively.

tively (M can be either pseudoscalar meson P or vector meson V). The explicit expressions of amplitudes $\mathcal{A}^{f,a}$ for $B_s\to PP,PV$ are listed in Appendixes A,B,C,D. A summary of the dynamical quantities a_i,b_i is given in Refs. [20–22].

III. INPUT PARAMETERS

Within the QCDF approach, the theoretical expressions of decay amplitudes depend on many input parameters including the standard model parameters (such as CKM matrix elements, quark masses), the renormalization scale μ, nonperturbative hadronic quantities (such as meson decay constants, form factors, and meson light cone distribution amplitudes), and so on. If quantitative predictions are to be made, these parameters must be specified. Using the renormalization group equations, it has been displayed in [33] that the dynamical quantities a_i are renormalization scale independent at the order of α_s. The numerical results in [20–22] also show that the renormalization scale dependence has been greatly reduced compared to the NF results. To illustrate this point, the dependence of coefficients $a_i(KK)$ on the renormalization scale μ is shown in Fig. 1 (where $a_i=a_{i,I}+a_{i,II}$, and $a_{i,I}$ contains the NF contributions and vertex and penguin corrections, while $a_{i,II}$ arises from the hard spectator interactions). It is believed that the residual scale dependence should be further reduced when higher order radiative corrections were considered. In the following, the QCD coefficients $a_{i,I}$ will be evaluated at the fixed scale $\mu=m_b$. Notice that hard spectator scattering $a_{i,II}$ and weak annihilation coefficients b_i should be evaluated at the scale of $\sqrt{m_b\Lambda_h}$ [20]. Other parameters are discussed below.

A. CKM matrix elements

The Wolfenstein parametrization [42] is widely used for the CKM matrix, which emphasizes the hierarchy among its elements by expressing them in terms of powers of $\lambda=|V_{us}|$:

$$V_{CKM}=\begin{pmatrix} 1-\lambda^2/2 & \lambda & A\lambda^3(\rho-i\eta) \\ -\lambda & 1-\lambda^2/2 & A\lambda^2 \\ A\lambda^3(1-\rho-i\eta) & -A\lambda^2 & 1 \end{pmatrix} + \mathcal{O}(\lambda^4). \tag{13}$$

The values of four Wolfenstein parameters (A, λ, ρ, and η) are given by several methods from the best knowledge of the experimental and theoretical inputs (for example, see Table II). Of the four CKM parameters, λ is to the accuracy of 1%. Within one standard deviation, the results of (A, $\bar{\rho}$, and $\bar{\eta}$) from different approaches [24,43–45] are virtually consistent with each other. In this paper, we shall take the values of Particle Data Group 2002 data [24] as the CKM parameter inputs: i.e., $\lambda=0.2236\pm0.0053$, $A=0.824\pm0.056$, $\bar{\rho}\equiv\rho(1-\lambda^2/2)=0.22\pm0.10$, $\bar{\eta}\equiv\eta(1-\lambda^2/2)=0.35\pm0.05$, and $\gamma=\arctan(\bar{\eta}/\bar{\rho})=(59\pm13)^\circ$.

However, it is not the right time to draw definite conclusions on the parameters ρ, η, and γ. Some interesting hints seem to favor $\gamma\gtrsim90^\circ$, which is in conflict with the data in Table II. For example, it is possible to put a constraint on the angle γ from a global analysis of B decays. Neglecting annihilation contributions, Bargiotti *et al.* [46] obtain the bound $|\gamma-90^\circ|>21^\circ$ at 95% C.L. from $B\to K\pi$ decay rates and CP asymmetries with SU(3) symmetry. Beneke *et al.* [20,47] make a global fit of $B\to\pi\pi$, $K\pi$ decays with the QCDF

approach, and their fit tends to favor $\gamma > 90°$. We extend the work of Beneke *et al.* [20,47] to include all $B \to PP, PV$ channels; the best fit of our global analysis gives $\lambda = 0.22$, $A = 0.82$, $\bar{\rho} = 0.086$, $\bar{\eta} = 0.39$, and $\gamma = 78.8°$ [34]. For comparison, we shall also take the above values as the CKM matrix inputs.

B. Quark masses

There are two different classes of quark masses. One type is the pole mass for constituent quarks, which appears in the penguin loop corrections with the functions $G_M(s_q)$ and $\hat{G}_M(s_q)$, where $s_q = m_q^2/m_b^2$. Here $G_M(s_q)$ and $\hat{G}_M(s_q)$ give partial information of strong phases, and its definitions can be found in [20]. In this paper, we take

$$m_u = m_d = m_s = 0, \quad m_c = 1.47 \ \text{GeV}, \quad m_b = 4.66 \ \text{GeV}. \tag{14}$$

The other is current quark mass which appears through the equations of motions and is renormalization scale dependent. Their values are [24]

$$\frac{1}{2}[\bar{m}_u(2 \ \text{GeV}) + \bar{m}_d(2 \ \text{GeV})] = (4.2 \pm 1.0) \ \text{MeV}, \tag{15}$$

$$\bar{m}_s(2 \ \text{GeV}) = (105 \pm 25) \ \text{MeV}, \tag{16}$$

$$\bar{m}_b(\bar{m}_b) = (4.26 \pm 0.15 \pm 0.15) \ \text{GeV}. \tag{17}$$

Here we would like to use their central values for discussion. Using the renormalization group equation, their corresponding values at the scale of $\mu = \mathcal{O}(m_b)$ can be obtained. Because the current masses of light quarks are determined with large uncertainties, for illustration we take

$$r_\chi = \frac{2m_K^2}{\bar{m}_b(\bar{m}_s + \bar{m}_q)} \simeq \frac{2\mu_P}{\bar{m}_b} \simeq r_\chi^\pi \simeq r_\chi^K \simeq r_\chi^{\eta^{(\prime)}}\left(1 - \frac{f_{\eta^{(\prime)}}^u}{f_{\eta^{(\prime)}}^s}\right), \tag{18}$$

which is numerically a good approximation. Note that $r_\chi^{\eta^{(\prime)}} = m_{\eta^{(\prime)}}^2/(\bar{m}_b \bar{m}_s)$.

C. Nonperturbative hadronic quantities

Nonperturbative hadronic quantities, such as meson decay constants, form factors, and meson light cone distribution amplitudes, appear as inputs in the QCDF formula (9). In principle, information about decay constants and form factors can be obtained form experiments and/or theoretical estimations. Now we specify these parameters. In this paper, we assume ideal mixing between ω and ϕ: i.e., $\omega = (u\bar{u} + d\bar{d})/\sqrt{2}$ and $\phi = s\bar{s}$. As to η and η', we take the convention in [15,31,48], using the Feldmann-Kroll-Stech mixing scheme for the decay constants, but neglecting the charm quark content in η and η' mesons, and the flavor singlet contributions [49] to the decay amplitudes which might need further discussions are not considered here:

$$\langle 0|\bar{q}\gamma_\mu\gamma_5 q|\eta^{(\prime)}(p)\rangle = \frac{i}{\sqrt{2}} f_{\eta^{(\prime)}}^q p_\mu,$$

$$\langle 0|\bar{s}\gamma_\mu\gamma_5 s|\eta^{(\prime)}(p)\rangle = i f_{\eta^{(\prime)}}^s p_\mu, \tag{19}$$

$$\frac{\langle 0|\bar{u}\gamma_5 u|\eta^{(\prime)}\rangle}{\langle 0|\bar{s}\gamma_5 s|\eta^{(\prime)}\rangle} = \frac{f_{\eta^{(\prime)}}^u}{f_{\eta^{(\prime)}}^s},$$

$$\langle 0|\bar{s}\gamma_5 s|\eta^{(\prime)}\rangle = -i\frac{m_{\eta^{(\prime)}}^2}{2m_s}(f_{\eta^{(\prime)}}^s - f_{\eta^{(\prime)}}^u), \tag{20}$$

$$f_\eta^u = \frac{f_q}{\sqrt{2}}\cos\phi, \quad f_\eta^s = -f_s \sin\phi, \quad F_0^{B_s\eta} = -\sin\phi F_0^{B_s\eta_{s\bar{s}}}, \tag{21}$$

$$f_{\eta'}^u = \frac{f_q}{\sqrt{2}}\sin\phi, \quad f_{\eta'}^s = f_s \cos\phi, \quad F_0^{B_s\eta'} = \cos\phi F_0^{B_s\eta'_{s\bar{s}}}, \tag{22}$$

where ϕ is the η-η' mixing angle. The numerical values of decay constants and form factors used in this paper are collected in Table III.

In this paper, we consider the contributions from chirally enhanced twist-3 light cone distribution amplitudes of a light pseudoscalar meson.[1] As to vector mesons, only the longitudinally polarized twist-2 terms are taken into account, and the effects from higher twist parts are neglected because they are power suppressed [51]. In our calculation, we shall take their asymptotic forms as default inputs, as displayed in [20,22,52]: i.e., for a light pseudoscalar meson, we have

$$\langle P(k)|\bar{q}(z_2)q(z_1)|0\rangle = \frac{if_P}{4}\int_0^1 dx e^{i(xk\cdot z_2 + \bar{x}k\cdot z_1)} \times\left\{ \not{k}\gamma_5\Phi_P(x) - \mu_P\gamma_5 \times\left[\Phi_P^p(x) - \sigma_{\mu\nu}k^\mu z^\nu\frac{\Phi_P^\sigma(x)}{6}\right]\right\}, \tag{23}$$

$$\text{twist-2 asymptotic forms: } \Phi_P(x) = 6x\bar{x},$$

$$\text{twist-3 asymptotic forms: } \Phi_P^p(x) = 1,$$

$$\Phi_P^\sigma(x) = 6x\bar{x}, \tag{24}$$

[1]The asymptotic form of leading twist distribution amplitude is valid for $\mu \to \infty$. For finite values of the renormalization scale, it is conventional to employ an expansion in Gegenbauer polynomials:

$$\Phi_P(x) = 6x\bar{x}\left[1 + \sum_{n=1}^{\infty}\alpha_n(\mu)C_n^{(3/2)}(\bar{x} - x)\right].$$

The Gegenbauer moments $\alpha_n(\mu)$ are multiplicatively renormalized. In the later discussion, this expansion is truncated at $n = 2$.

TABLE II. The values of the Wolfenstein parameters A, λ, ρ, and η.

Refs.	[43]	[44]	[45]	[24]
λ	0.2237 ± 0.0033	0.2221 ± 0.0041	0.2210 ± 0.0020	0.2236 ± 0.0053[a]
A	0.819 ± 0.040[b]	$0.763\sim0.905$	0.831 ± 0.022[b]	0.824 ± 0.056[b]
$\bar{\rho}$	0.224 ± 0.038	$0.07\sim0.37$	0.173 ± 0.046	0.22 ± 0.10
$\bar{\eta}$	0.317 ± 0.040	$0.26\sim0.49$	0.357 ± 0.027	0.35 ± 0.05
γ	$(54.8\pm6.2)^\circ$	$37^\circ\sim80^\circ$	$(63.5\pm7.0)^\circ$	$(59\pm13)^\circ$

[a]Determined from the measurements of $|V_{ud}|=0.9734\pm0.0008$ and $|V_{us}|=0.2196\pm0.0026$.
[b]$A=|V_{cb}|/\lambda$, and $|V_{cb}|=(40.6\pm0.8)\times10^{-3}$ [45], $(41.2\pm2.0)\times10^{-3}$ [24].

where f_P is a decay constant; $z=z_2-z_1$, and $\bar{x}=1-x$.

For a longitudinally polarized vector meson, we have [52,53]

$$\langle 0|\bar{q}(0)\gamma_\mu q(z)|V(k,\lambda)\rangle = k_\mu \frac{\epsilon^\lambda\cdot z}{k\cdot z} f_V m_V \times\int_0^1 dx e^{-ixk\cdot z}\Phi_V^\parallel(x), \quad (25)$$

$$\text{twist-2 asymptotic forms: } \Phi_V^\parallel(x)=6x\bar{x}, \quad (26)$$

where ϵ is the polarization vector, and $\epsilon_\parallel=k/m_V$.

The light cone distribution amplitudes of B meson is less clear. But it is intuitive that at the scale of $\mu\sim\mathcal{O}(m_b)$ and smaller, the distribution amplitudes of the B meson should be very asymmetric because the spectator quark in the B meson is not energetic. Fortunately, the B meson light cone distribution amplitudes appears only in the integral of hard spectator scattering kernels within the QCDF approach; therefore, for phenomenological analysis, we do not need to know the explicit expression of the B meson wave function. Here, we would like to parametrize this integral as [20]

$$\int_0^1\frac{d\xi}{\xi}\Phi_B(\xi)\equiv\frac{m_B}{\lambda_B}, \quad \lambda_B=(350\pm150)\ \text{MeV}. \quad (27)$$

For the logarithmic divergence appearing in the hard spectator scattering and annihilation contributions, we will follow the parametrization of Ref. [20]:

$$X=\int_0^1\frac{dx}{x}=(1+\varrho e^{i\phi})\ln\frac{m_b}{\Lambda_h}, \quad \varrho\leqslant1, \quad 0^\circ\leqslant\phi\leqslant360^\circ. \quad (28)$$

TABLE III. Values of meson decay constants, form factors, and η-η' mixing parameters.

$F_0^{B_sK}$	0.274	[28]	f_π	131 MeV	[24]	f_{K^*}	214 MeV	[15]
$F_0^{B_s\eta_{ss}^-}$	0.335	[28]	f_K	160 MeV	[24]	f_ρ	210 MeV	[15]
$F_0^{B_s\eta_{ss}^{\prime-}}$	0.282	[28]	f_q	$1.07\,f_\pi$	[48]	f_ω	195 MeV	[15]
$A_0^{B_sK^*}$	0.236	[28]	f_s	$1.34\,f_\pi$	[48]	f_ϕ	233 MeV	[15]
$A_0^{B_s\phi}$	0.272	[28]	ϕ	39.3°	[48]	f_{B_s}	236 MeV	[50]

In Ref. [34] we made a global analysis of $B_{u,d}\to PP,PV$ decays using the CKMFITTER package [44] and obtained the best-fit values of theoretical inputs including X_A. It should be reasonable to assume that X_A for $B_{u,d}$ decays is equal to that of B_s decays. Therefore, in numerical calculations, we take their default values as

decay modes	ϱ_H	ϕ_H	ϱ_A [34]	ϕ_A [34]	Λ_h [20]
$B_s\to PP$	0	0	0.5	10°	0.5 GeV
$B_s\to PV$	0	0	1.0	-30°	0.5 GeV

where (ϱ_H,ϕ_H) and (ϱ_A,ϕ_A) are related to the contributions from hard spectator scattering and weak annihilations, respectively.

IV. BRANCHING RATIOS

The branching ratios for charmless $B_s\to PP,PV$ decays in B_s meson rest frame can be written as

$$BR(B_s\to M_1M_2)=\frac{\tau_{B_s}}{8\pi}\frac{|p|}{m_{B_s}^2}|\mathcal{A}(B_s\to M_1M_2)|^2, \quad (29)$$

where

$$|p|=\frac{\sqrt{[m_{B_s}^2-(m_{M_1}+m_{M_2})^2][m_{B_s}^2-(m_{M_1}-m_{M_2})^2]}}{2m_{B_s}}. \quad (30)$$

The lifetime and mass for B_s meson are $\tau_{B_s}=1.461$ ps, and $m_{B_s}=5369.6$ MeV [24]. Formally the mass scale of light final states is of the order of Λ_{QCD} in the heavy quark limits, and power corrections of order Λ_{QCD}/m_b could be consistently neglected within the QCDF framework if there is no chiral enhanced factor, so $|p|\simeq m_{B_s}/2$.

The numerical results of CP-averaged branching ratios for B_s decays are listed in Tables IV and V. We have evaluated the vertex and penguin corrections at the scale of $\mu=m_b$, while hard spectator scattering and weak annihilation contributions at the scale of $\mu_h=\sqrt{m_b\Lambda_h}$. Two sets of input values of CKM parameters are used for comparison. The numbers in the $BR1$ columns are calculated within the NF framework: i.e., kernels $T^I=1$ and $T^{II}=0$. The numbers in the $BR2$

TABLE IV. The *CP*-averaged branching ratios (in the unit of 10^{-6}) of decays $B_s \to PP$ calculated with the default input parameters. The numbers in columns 2–5 (see the text for their meanings) are computed with $A=0.824$, $\lambda=0.2236$, $\bar{\rho}=0.22$, $\bar{\eta}=0.35$, and $\gamma=59°$, while the numbers in columns 6–9 are computed with $A=0.82$, $\lambda=0.22$, $\bar{\rho}=0.086$, $\bar{\eta}=0.39$, and $\gamma=78.8°$.

Decay modes	NF	QCDF			NF	QCDF		
	$BR1$	$BR2$	$BR3$	$BR4$	$BR1$	$BR2$	$BR3$	$BR4$
$\bar{B}_s^0 \to K^0 \bar{K}^0$	8.452	11.99	10.94	25.03	7.746	11.00	10.03	22.95
$\bar{B}_s^0 \to K^0 \pi^0$	0.187	0.120	0.271	0.356	0.243	0.144	0.341	0.484
$\bar{B}_s^0 \to K^0 \eta$	0.107	0.047	0.159	0.170	0.123	0.054	0.167	0.193
$\bar{B}_s^0 \to K^0 \eta'$	0.429	0.434	0.953	1.544	0.391	0.480	0.889	1.540
$\bar{B}_s^0 \to \pi^0 \pi^0$	—	—	—	0.051	—	—	—	0.050
$\bar{B}_s^0 \to \pi^0 \eta$	0.052	0.065	0.052	0.056	0.058	0.061	0.059	0.059
$\bar{B}_s^0 \to \pi^0 \eta'$	0.055	0.069	0.053	0.051	0.061	0.064	0.062	0.063
$\bar{B}_s^0 \to \eta \eta$	4.363	6.505	5.160	11.64	3.901	5.957	4.625	10.54
$\bar{B}_s^0 \to \eta \eta'$	8.944	11.44	15.77	30.24	8.176	10.49	14.42	27.61
$\bar{B}_s^0 \to \eta' \eta'$	4.589	4.967	13.50	27.53	4.293	4.573	12.58	25.55
$\bar{B}_s^0 \to K^+ \pi^-$	9.633	10.58	9.292	9.683	7.304	7.943	6.963	7.045
$\bar{B}_s^0 \to K^+ K^-$	6.729	9.652	8.884	21.41	7.582	10.58	9.699	22.14
$\bar{B}_s^0 \to \pi^+ \pi^-$	—	—	—	0.101	—	—	—	0.099

columns are calculated within the QCDF framework and $BR2 \propto |\mathcal{A}^f|^2$, but without contributions from hard spectator scattering interactions and annihilation topologies: i.e., coefficients $a_i = a_{i,I}$, $a_{i,II} = b_i = 0$. The numbers in the $BR3$ columns are calculated within the QCDF framework, including chirally enhanced hard spectator scattering contributions, but without annihilation effects: i.e., $BR3 \propto |\mathcal{A}^f|^2$, $a_i = a_{i,I} + a_{i,II}$, $b_i = 0$. The numbers in the $BR4$ columns are calculated within the QCDF framework, including chirally enhanced hard spectator scattering contributions and annihilation effects: i.e., $BR4 \propto |\mathcal{A}^f + \mathcal{A}^a|^2$. Some remarks are in order.

(i) Only several interesting decay modes with large branching ratios, such as $B_s \to K^{(*)} K, K^{(*)\pm} \pi^{\mp}, K^{\pm} \rho^{\mp}, \eta^{(\prime)} \eta^{(\prime)}$, might be observed in the near future. Branching ratios of other decay modes are small, not exceeding 2×10^{-6}. Especially for decays $B_s \to \pi \eta^{(\prime)}, \pi \phi, \rho \eta^{(\prime)}, \omega \eta^{(\prime)}$ whose tree contributions are suppressed by both CKM factor and color, and penguin contributions which are electroweak coefficient a_9 dominant, their *CP*-averaged branching ratios are very small, around $\mathcal{O}(10^{-7})$. As to these power-suppressed pure weak annihilation decays, such as $B_s \to \pi\pi, \pi\rho, \pi\omega$, their branching ratios are extremely small, around $\mathcal{O}(10^{-8})$.

(ii) For those $b \to s$ transition decay modes, such as $B_s \to \eta^{(\prime)} \eta^{(\prime)}, K^{(*)} K$, their tree contributions are CKM suppressed, so penguin contributions are either competitive with the tree part or even dominant in the decay amplitudes. Since ''nonfactorizable'' effects contribute a large portion to penguin coefficients $a_{4,6}$, the predictions of QCDF are substantially larger than those of NF. In addition, the annihilation coefficients b_1 and/or b_3 contribute to these decay amplitudes, and the numbers in Tables IV and V show that weak annihilation contributions could be sizable ($\gtrsim 50\%$) for these decay channels. For those $b \to d$ transition decay modes, such as $B_s \to K^{(*)\pm} \pi^{\mp}, K^{\pm} \rho^{\mp}$, they are a_1 dominant which receives small radiative corrections, so the numbers in Tables IV and V show no large difference between the results of the QCDF approach and those of the NF approach.

(iii) There are hierarchies among some decay modes, such as

$$BR(\bar{B}_s^0 \to K^+ K^-) > BR(\bar{B}_s^0 \to K^+ K^{*-}) > BR(\bar{B}_s^0 \to K^- K^{*+}), \tag{31}$$

$$BR(\bar{B}_s^0 \to \bar{K}^0 K^0) > BR(\bar{B}_s^0 \to K^0 \bar{K}^{*0}) > BR(\bar{B}_s^0 \to \bar{K}^0 K^{*0}), \tag{32}$$

$$BR(\bar{B}_s^0 \to K^+ \pi^-) > BR(\bar{B}_s^0 \to K^{*+} \pi^-). \tag{33}$$

There are two reasons for the above relations. One is that the penguin contributions are important or even dominant for these decays. Their decay amplitudes involve the QCD penguin parameters a_4 and a_6 in the form of $a_4 + R a_6$, where $R>0$ for $B_s \to PP$ decays, and $R=0$ ($R<0$) for $B_s \to PV$ decays with $B \to P$ ($B \to V$) transition, respectively, as stated in [31]. The other is for the second inequality of Eq. (31) and Eq. (32); it is simply due to the fact that $f_{K^*} F_1^{B_s^0 \to K} > f_K A_0^{B_s^0 \to K^*}$. The numerical results in Tables IV and V confirm the above relations in general. Here we would like to point out that because the weak annihilation parameters $A_3^f(P,V) = -A_3^f(V,P)$ (the definition of A_3^f can be found in [20,22]) and the combination of $b_1 + b_3$ (or $b_3 + 2b_4$) is destructive for decays $\bar{B}_s^0 \to K^+ K^{*-}$ (or $K^0 \bar{K}^{*0}$) and construc-

TABLE V. The *CP*-averaged branching ratios (in the unit of 10^{-6}) of decays $B_s \to PV$ calculated with the default input parameters. The captions are the same as in Table IV.

Decay modes	NF	QCDF			NF	QCDF		
	$BR1$	$BR2$	$BR3$	$BR4$	$BR1$	$BR2$	$BR3$	$BR4$
$\bar{B}_s^0 \to K^0 \bar{K}^{*0}$	2.178	3.115	2.428	6.788	1.996	2.860	2.229	6.233
$\bar{B}_s^0 \to \bar{K}^0 K^{*0}$	0.364	0.512	0.715	5.778	0.334	0.469	0.655	5.295
$\bar{B}_s^0 \to K^+ K^{*-}$	1.831	2.461	1.985	5.277	2.614	3.395	2.763	6.555
$\bar{B}_s^0 \to K^- K^{*+}$	1.175	1.463	1.631	7.748	0.803	1.001	1.127	6.041
$\bar{B}_s^0 \to \pi^+ \rho^-$	—	—	—	0.014	—	—	—	0.010
$\bar{B}_s^0 \to \pi^- \rho^+$	—	—	—	0.014	—	—	—	0.010
$\bar{B}_s^0 \to K^0 \rho^0$	0.369	0.080	0.575	0.596	0.350	0.075	0.529	0.650
$\bar{B}_s^0 \to K^0 \omega$	0.421	0.149	0.639	0.745	0.291	0.139	0.480	0.519
$\bar{B}_s^0 \to K^0 \phi$	0.027	0.047	0.078	0.340	0.033	0.058	0.096	0.413
$\bar{B}_s^0 \to \pi^0 K^{*0}$	0.135	0.044	0.208	0.301	0.094	0.040	0.148	0.211
$\bar{B}_s^0 \to \pi^0 \rho^0$	—	—	—	0.014	—	—	—	0.010
$\bar{B}_s^0 \to \pi^0 \omega$	—	—	—	0.002	—	—	—	0.002
$\bar{B}_s^0 \to \pi^0 \phi$	0.086	0.106	0.085	—	0.095	0.100	0.096	—
$\bar{B}_s^0 \to \eta K^{*0}$	0.119	0.107	0.148	0.353	0.165	0.129	0.196	0.514
$\bar{B}_s^0 \to \eta' K^{*0}$	0.064	0.024	0.172	0.234	0.044	0.019	0.123	0.176
$\bar{B}_s^0 \to \eta \rho^0$	0.121	0.151	0.122	0.130	0.135	0.142	0.139	0.137
$\bar{B}_s^0 \to \eta' \rho^0$	0.128	0.160	0.126	0.123	0.143	0.150	0.148	0.153
$\bar{B}_s^0 \to \eta \omega$	0.037	0.010	0.025	0.006	0.047	0.009	0.017	0.005
$\bar{B}_s^0 \to \eta' \omega$	0.040	0.010	0.040	0.075	0.050	0.010	0.027	0.051
$\bar{B}_s^0 \to \eta \phi$	0.286	0.417	0.088	0.166	0.240	0.385	0.084	0.166
$\bar{B}_s^0 \to \eta' \phi$	0.002	0.134	0.149	0.024	0.003	0.120	0.155	0.028
$\bar{B}_s^0 \to K^+ \rho^-$	23.68	25.60	22.38	22.85	19.00	20.45	17.92	17.77
$\bar{B}_s^0 \to \pi^- K^{*+}$	6.641	7.098	6.233	6.197	5.696	6.116	5.412	5.737

tive for decays $\bar{B}_s^0 \to K^- K^{*+}$ (or $\bar{K}^0 K^{*0}$), large contributions from weak annihilation topologies might affect the above hierarchies.

(iv) It is interesting to note that $B_s \to \eta^{(\prime)} \eta^{(\prime)}$ decays have large branching ratios. In fact, their SU(3) counterpart $B_{u,d} \to K \eta'$ has been reported to have the largest branching ratios among the two-body charmless rare B decays:

decay modes	CLEO [54]	BABAR [2]	Belle [6]
$BR(B_d \to K_s \eta') \times 10^6$	$89^{+18}_{-16} \pm 9$	$42^{+13}_{-11} \pm 4$	$55^{+19}_{-16} \pm 8$
$BR(B_u \to K^{\pm} \eta') \times 10^6$	$89^{+10}_{-9} \pm 9$	$70 \pm 8 \pm 4$	$79^{+12}_{-11} \pm 9$

The surprisingly large branching ratios for $B_{u,d} \to K \eta'$ decays have triggered intense theoretical interests (see, for example, Refs. [55–58]). It is generally believed that this problem is related to the axial anomaly in QCD, but the dynamical details remain unclear. In Refs. [57,58], the digluon fusion mechanism (η' couples to two off-shell gluons, one from the spectator quark, the other from the b quark decay vertex) was proposed to account for the large branching ratios of $B_{u,d} \to K \eta'$. It is further shown in [17] that the QCDF approach including the digluon fusion mechanism can give a good explanation of the experimental data. But most recently, Beneke and Neubert discussed in detail the exclusive $B_{u,d} \to \eta^{(\prime)} K^{(*)}$ decays using the QCDF approach [49]. They found that it is not the digluon fusion mechanism, but the constructive or destructive interference of nonsinglet penguin amplitudes playing the key role in exclusive $B \to \eta^{(\prime)} K^{(*)}$ decays. In their paper, a new kind of parametrization is proposed for the form factor $F^{B \eta^{(\prime)}}$ which is crucial to qualitatively account for the large experimental measurements. But this point might need further investigation. In this paper, we simply consider the conventional contributions to $B_s \to \eta^{(\prime)} \eta^{(\prime)}$ decays, while leaving further discussions to future work.

(v) Generally speaking, the numerical results of the branching ratios of B_s decays are dependent on the input values of the CKM matrix parameters, but it is clear that only those a_1-dominated $b \to d$ decays and those with large interference between tree and penguin contributions, such as $B_s \to K^{\pm} \pi^{\mp}$, $K^{\pm} K^{(*)\mp}$, are sensitive to the CKM angle γ.

Of course, theoretical uncertainties from input parameters (such as the CKM matrix elements, light quark masses, form factors, meson light cone distribution amplitudes, and so on)

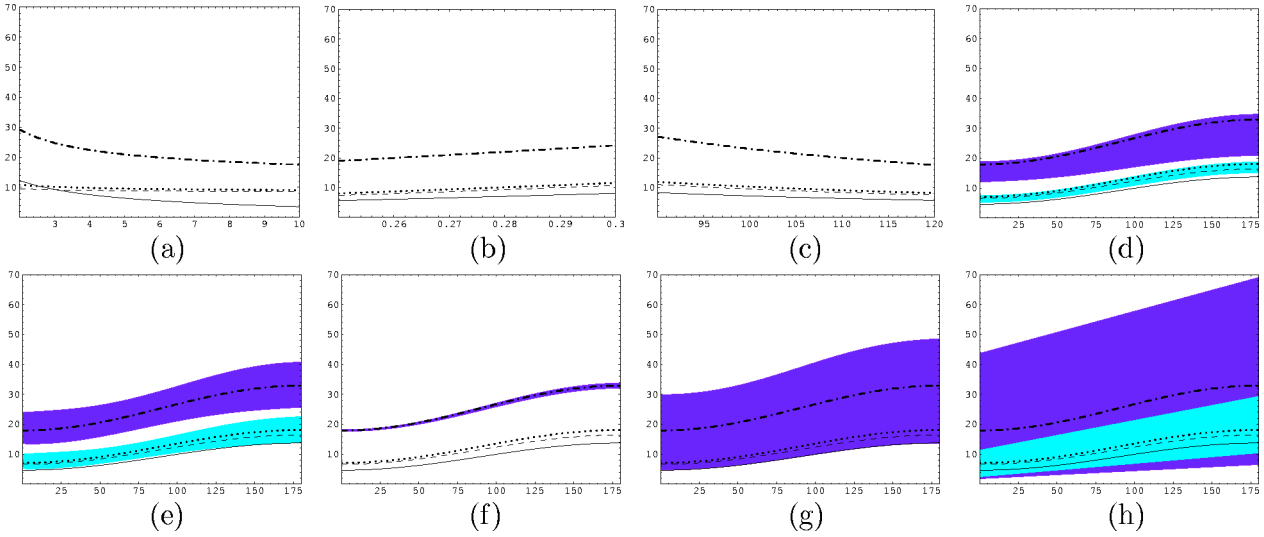

FIG. 2. *CP*-averaged branching ratios of decay $B_s \to K^{\pm}K^{\mp}$ (vertical axes, in units of 10^{-6}) versus the renormalization scale μ (horizontal axes, in units of GeV, and the scale $\mu_h = \sqrt{\Lambda_h \mu}$ for contributions from chirally enhanced hard spectator scattering and annihilation interactions) in (a), the form factor $F_0^{B_s \to K}$ in (b), the light quark mass $\overline{m}_s(2\ \mathrm{GeV})$ [in units of MeV, and keeping $\overline{m}_q(2\ \mathrm{GeV})/\overline{m}_s(2\ \mathrm{GeV}) = 4.2/105$ fixed] in (c), and the CKM angle γ (in units of degree) in (d)–(h), respectively. The legends on lines and bands are explained in the text.

should be taken into account when discussing B_s decays. For $B_{u,d}$ decays, it has been investigated in detail in Refs. [20–22]. In Figs. 2–5, we show the dependence of the *CP*-averaged branching ratios of decays $B_s \to K^{\pm}K^{\mp}$, $K^{\pm}\pi^{\mp}$, $\overline{K}^0 K^0$, and $\pi^{\pm}\pi^{\mp}$ on input parameters. In each plot, the solid lines denote the results of $BR1$ with the NF approach: i.e., kernels of $T_i^I = 1$, $T_i^{II} = 0$. Other lines and bands denote the results within the QCDF framework. The dotted lines and light gray bands correspond to the results of $BR2$: i.e., without contributions from chirally enhanced hard spectator scattering and annihilation interactions, $a_i = a_{i,I}$, $a_{i,II} = b_i = 0$. The dashed lines denote the results of $BR3$: i.e., including the corrections of chirally enhanced hard spectator scattering, but without annihilation effects, $a_i = a_{i,I} + a_{i,II}$, $b_i = 0$. The dot-dashed lines and dark bands denote the results of $BR4$: i.e., including contributions from chirally enhanced hard spectator scattering and annihilation interactions. The gray bands in Fig. 3 are the overlapping part of the light and dark gray bands. The bands in Fig. (#d) denote the uncertainties from parameters λ_B, and the Gegenbauer moments of the twist-2 light cone distribution amplitudes of final states [here Fig. (#d) means Fig. (d) in all Figs. 2–5; it is the same below]; the bands in Fig. (#e) denote the uncertainties from the CKM elements A, λ, and $|V_{ub}|$; the bands in Figs. (#f) and (#g) correspond to the uncertainties form parameters of X_H and X_A, respectively; the bands in Fig. (#h) denote the overall uncertainties: i.e., the combinations of Figs. (#a)–(#g). We assign a 10% uncertainty to form factor and light

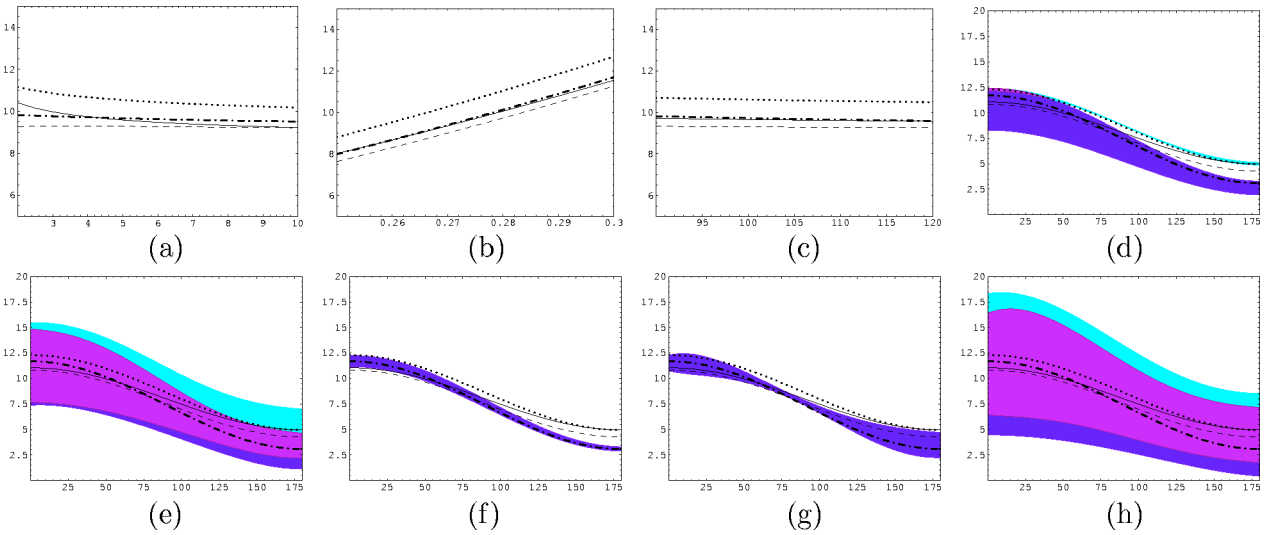

FIG. 3. *CP*-averaged branching ratios of decay $B_s \to K^{\pm}\pi^{\mp}$ (vertical axes, in units of 10^{-6}). The legends are the same as in Fig. 2.

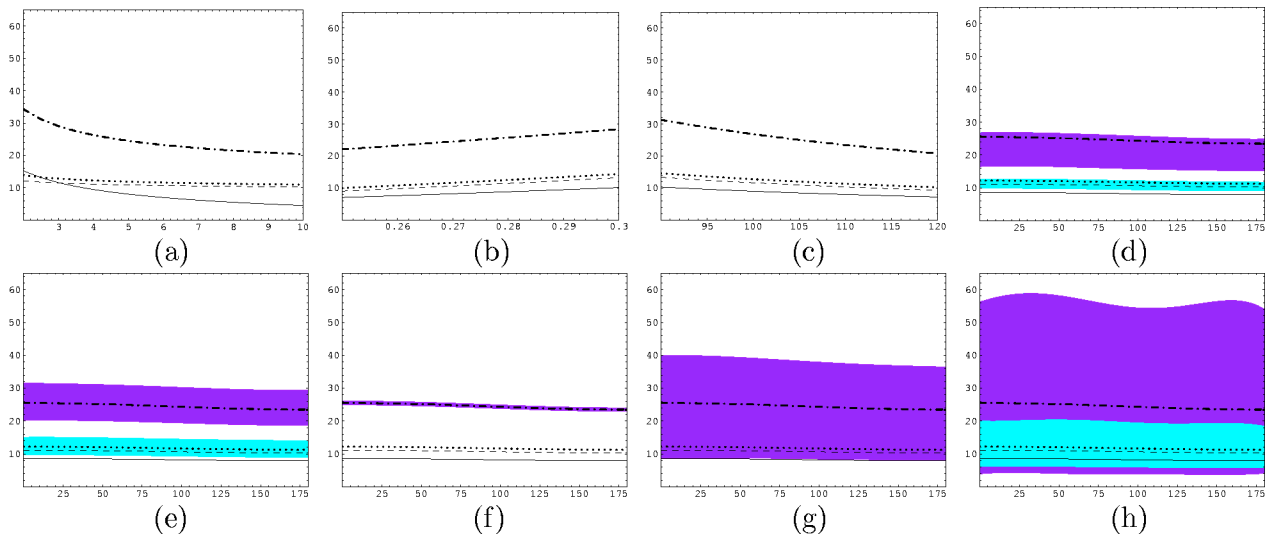

FIG. 4. *CP*-averaged branching ratios of decay $B_s \to K^0 \overline{K^0}$ (vertical axes, in units of 10^{-6}). The legends are the same as in Fig. 2.

quark masses, $F_0^{B_s \to K} = 0.250$–0.300, $\overline{m}_s(2\ \mathrm{GeV}) = 90$–$120$ MeV [keeping the ratio of light quark masses fixed, $\overline{m}_q(2\ \mathrm{GeV})/\overline{m}_s(2\ \mathrm{GeV}) = 4.2/105$]; the regions of other parameters are scale $\mu = 2$–10 GeV for coefficients of $a_{i,I}$ (the corresponding scale μ_h for $a_{i,II}$ and b_i is $\sqrt{\mu \Lambda_h}$ [20]), $|V_{ub}| = (3.6 \pm 0.7) \times 10^{-3}$ [24], and the Gegenbauer moments $\alpha_1^K = 0.3 \pm 0.3$, $\alpha_2^K = 0.1 \pm 0.3$, $\alpha_1^\pi = 0$, $\alpha_2^\pi = 0.1 \pm 0.3$ [20]. A number of observations are in order.

(i) From Fig. (#a), we can see that the renormalization scale dependence of the QCDF results without weak annihilation (dotted and dashed lines) has been greatly reduced compared to their corresponding NF counterpart (solid lines). The weak annihilation contributions are renormalization scale dependent and bring large uncertainties, although they are power suppressed within the QCDF framework.

(ii) For a_1 dominant decays, such as $B_s \to K^\pm \pi^\mp$, there is an obvious difference between the results of $BR2$ and $BR3$. The CKM elements and form factor can bring large theoretical uncertainties because ''nonfactorizable'' contributions are suppressed by either α_s or Λ_{QCD}/m_b within the QCDF framework, but in principle, these uncertainties could be reduced by the ratios of branching ratios. In addition, uncertainties form parameters of λ_B, Gegenbauer moments $\alpha_n^{K,\pi}$ are also large (see Fig. 3).

(iii) For those penguin dominant decays, such as $B_s \to \overline{K^0} K^0$, and those with a large interference between tree and penguin contributions, such as $B_s \to K^\pm K^\mp$, the power-suppressed annihilation contributions are important which lead to a large renormalization scale dependence, but uncertainties from parameter X_A are also sizable (see Figs. 2 and 4).

(iv) $B_s \to \pi^+ \pi^-$ decay is a pure annihilation process. Its amplitude is free from transition form factors and hard spectator scattering corrections. Hence the dominant theoretical uncertainties come from the annihilation parameter of X_A and the renormalization scale (see Fig. 5). Experimentally, it is worth searching for such a pure annihilation process which may be helpful to learn more about the annihilation mecha-

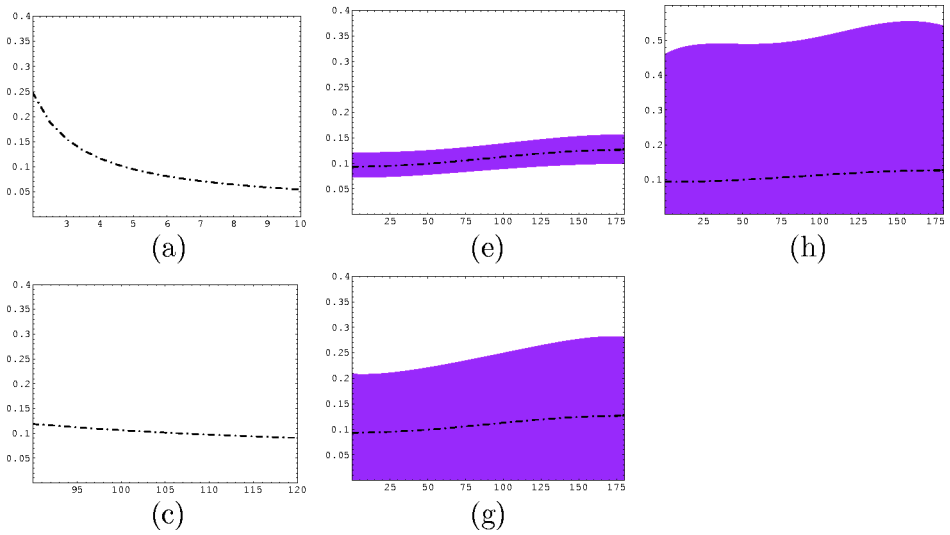

FIG. 5. *CP*-averaged branching ratios of decay $B_s \to \pi^\pm \pi^\mp$ (vertical axes, in units of 10^{-6}). The legends are the same as in Fig. 2.

nism and to provide some useful information about final state interactions.

(v) From Fig. (#h), we can see that there exists sizable theoretical uncertainties, which make it nontrivial to extract helpful information on the CKM matrix parameters. But the uncertainties from the hard spectator parameter X_H are very small—Fig. (#f). Those a_1-dominated $b\to d$ decays, such as $B_s\to K^\pm\pi^\mp$, and those with a large interference between tree and penguin contributions, such as $B_s\to K^\pm K^\mp$, are sensitive to the CKM angle γ. These channels are predicted to have large branching ratios and should be observed in the future.

V. *CP* ASYMMETRIES

CP-violating asymmetries for B_s decays have been studied in [29]. In this paper, we shall evaluate them with the QCDF approach. In principle, calculations of the *CP*-violating asymmetries for B_s are similar with those for B_d decays. As a result of flavor-changing interactions, $\overline{B}_s^0$ and B_s^0 can oscillate into each other with time evolution. The time-dependent *CP* asymmetry $\mathcal{A}_{CP}$ for B_s decays is defined as

$$\mathcal{A}_{CP}(t)=\frac{\Gamma(\overline{B}_s^0(t)\to\overline{f})-\Gamma(B_s^0(t)\to f)}{\Gamma(\overline{B}_s^0(t)\to\overline{f})+\Gamma(B_s^0(t)\to f)}. \tag{34}$$

As discussed previously in Refs. [15,21,22], the $B_s\to PP,PV$ decays can be classified into three cases according to the properties of the final states.

(i) Case I: $B_s^0\to f$, $\overline{B}_s^0\to\overline{f}$, but $B_s^0\not\to\overline{f}$, $\overline{B}_s^0\not\to f$, for example, $\overline{B}_s^0\to K^+\rho^-,\pi^-K^{*+},\ldots$, the *CP*-violating asymmetry for these decays is time independent,

$$\mathcal{A}_{CP}=\frac{\Gamma(\overline{B}_s^0\to\overline{f})-\Gamma(B_s^0\to f)}{\Gamma(\overline{B}_s^0\to\overline{f})+\Gamma(B_s^0\to f)}. \tag{35}$$

(ii) Case II: $B_s^0\to(f=\overline{f})\leftarrow\overline{B}_s^0$, for example, $B_s\to K^\pm K^\mp,\eta^{(\prime)}\eta^{(\prime)},\ldots$, the time-integrated *CP*-violating asymmetry for these decays is

$$\mathcal{A}_{CP}=\frac{1}{1+x_s^2}a_{\epsilon'}+\frac{x_s}{1+x_s^2}a_{\epsilon+\epsilon'}, \tag{36}$$

$$a_{\epsilon'}=\frac{1-|\lambda_{CP}|^2}{1+|\lambda_{CP}|^2},\quad a_{\epsilon+\epsilon'}=\frac{-2\,\mathrm{Im}(\lambda_{CP})}{1+|\lambda_{CP}|^2},$$

$$\lambda_{CP}=\frac{V_{ts}V_{tb}^*}{V_{ts}^*V_{tb}}\frac{\mathcal{A}(\overline{B}_s^0(0)\to\overline{f})}{\mathcal{A}(B_s^0(0)\to f)}, \tag{37}$$

where $a_{\epsilon'}$ and $a_{\epsilon+\epsilon'}$ are direct and mixing-induced *CP*-violating asymmetries, respectively. The mixing parameter $x_s=\Delta m_{B_s}/\Gamma_{B_s}$ is considerably large for the B_s system, $x_s>19.0$ at 95% C.L. [24]. In our calculation, we shall take the preferred value in the standard model, $x_s\simeq 20$ [59]. Clearly, the *CP*-violating asymmetry $\mathcal{A}_{CP}$ should be very small because $a_{\epsilon'}$ and $a_{\epsilon+\epsilon'}$ in Eq. (36) are strongly suppressed by $1/x_s^2$ and $1/x_s$, respectively.

(iii) Case III: $B_s^0\to(f,\overline{f})\leftarrow\overline{B}_s^0$, for example, $B_s\to(K_S^0\overline{K}^{*0},K_S^0K^{*0}),(K^+K^{*-},K^-K^{*+}),(\pi^+\rho^-,\pi^-\rho^+)$. Analogous to the notation for B_d decays in [15], the time-dependent decay widths for this case of B_s decays are written as

$$\Gamma(B_s^0(t)\to f)=\frac{e^{-\Gamma_{B_s}t}}{2}(|g|^2+|h|^2)[1+a_{\epsilon'}\cos(\Delta m_{B_s}t)+a_{\epsilon+\epsilon'}\sin(\Delta m_{B_s}t)], \tag{38}$$

$$\Gamma(\overline{B}^0(t)\to\overline{f})=\frac{e^{-\Gamma_{B_s}t}}{2}(|\overline{g}|^2+|\overline{h}|^2)[1-a_{\overline{\epsilon}'}\cos(\Delta m_{B_s}t)-a_{\epsilon+\overline{\epsilon}'}\sin(\Delta m_{B_s}t)], \tag{39}$$

$$\Gamma(B^0(t)\to\overline{f})=\frac{e^{-\Gamma_{B_s}t}}{2}(|\overline{g}|^2+|\overline{h}|^2)[1+a_{\overline{\epsilon}'}\cos(\Delta m_{B_s}t)+a_{\epsilon+\overline{\epsilon}'}\sin(\Delta m_{B_s}t)], \tag{40}$$

$$\Gamma(\overline{B}^0(t)\to f)=\frac{e^{-\Gamma_{B_s}t}}{2}(|g|^2+|h|^2)[1-a_{\epsilon'}\cos(\Delta m_{B_s}t)-a_{\epsilon+\epsilon'}\sin(\Delta m_{B_s}t)], \tag{41}$$

where

$$g=\mathcal{A}(B_s^0(0)\to f),\quad \overline{g}=\mathcal{A}(\overline{B}_s^0(0)\to\overline{f}), \tag{42}$$

$$h=\mathcal{A}(\overline{B}_s^0(0)\to f),\quad \overline{h}=\mathcal{A}(B_s^0(0)\to\overline{f}), \tag{43}$$

and, with $q/p=V_{ts}V_{tb}^*/V_{ts}^*V_{tb}$,

$$a_{\epsilon'}=\frac{|g|^2-|h|^2}{|g|^2+|h|^2},\quad a_{\epsilon+\epsilon'}=\frac{-2\,\mathrm{Im}[(q/p)\times(h/g)]}{1+|h/g|^2}, \tag{44}$$

$$a_{\overline{\epsilon}'}=\frac{|\overline{h}|^2-|\overline{g}|^2}{|\overline{h}|^2+|\overline{g}|^2},\quad a_{\epsilon+\overline{\epsilon}'}=\frac{-2\,\mathrm{Im}[(q/p)\times(\overline{g}/\overline{h})]}{1+|\overline{g}/\overline{h}|^2}. \tag{45}$$

Our numerical results of the *CP*-violating asymmetries for $B_s\to PP,PV$ decays are listed in Tables VI–IX, which are calculated with two sets of CKM matrix parameters within the QCDF framework. The numbers in the $a_{\epsilon'2}$, $a_{\epsilon+\epsilon'2}$, and $\mathcal{A}_{CP2}$ columns are computed with amplitude $\mathcal{A}^f$ and its corresponding *CP* conjugate parts $\overline{\mathcal{A}^f}$, but without contributions from hard spectator scattering interactions and annihilation topologies: i.e., coefficients $a_i=a_{i,I}$, $a_{i,II}=b_i=0$. The numbers in the $a_{\epsilon'3}$, $a_{\epsilon+\epsilon'3}$, and $\mathcal{A}_{CP3}$ columns are computed with amplitudes $\mathcal{A}^f$ and $\overline{\mathcal{A}^f}$, including chirally enhanced hard spectator scattering contributions, but without considering annihilation effects: i.e., $a_i=a_{i,I}+a_{i,II}$, $b_i=0$. The numbers in the $a_{\epsilon'4}$, $a_{\epsilon+\epsilon'4}$, and $\mathcal{A}_{CP4}$ columns are com-

TABLE VI. The *CP*-violating asymmetry parameters $a_{\epsilon'}$ and $a_{\epsilon+\epsilon'}$ for $B_s \to PP$ decays (in units of percent) with the QCDF approach, using the default input parameters. The numbers in columns 2–7 (see the text for their meaning) are computed with $A=0.824$, $\lambda=0.2236$, $\bar{\rho}=0.22$, $\bar{\eta}=0.35$, and $\gamma=59°$, while the numbers in columns 8–13 are computed with $A=0.82$, $\lambda=0.22$, $\bar{\rho}=0.086$, $\bar{\eta}=0.39$, and $\gamma=78.8°$.

Modes	$a_{\epsilon'2}$	$a_{\epsilon'3}$	$a_{\epsilon'4}$	$a_{\epsilon+\epsilon'2}$	$a_{\epsilon+\epsilon'3}$	$a_{\epsilon+\epsilon'4}$	$a_{\epsilon'2}$	$a_{\epsilon'3}$	$a_{\epsilon'4}$	$a_{\epsilon+\epsilon'2}$	$a_{\epsilon+\epsilon'3}$	$a_{\epsilon+\epsilon'4}$
$B_s \to K^0 \bar{K}^0$	−0.890	−0.934	−0.616	3.380	3.373	3.459	−0.971	−1.019	−0.672	3.662	3.655	3.749
$B_s \to K_S^0 \pi^0$	−67.36	−42.99	−45.96	−59.38	−8.221	−45.20	−56.18	−34.21	−33.79	−67.41	−64.41	−82.90
$B_s \to K_S^0 \eta$	−91.79	−34.86	−42.02	−31.66	47.26	25.62	−80.61	−33.19	−37.01	−53.37	−20.96	−40.51
$B_s \to K_S^0 \eta'$	58.20	38.50	32.86	−44.56	−5.939	−24.27	52.61	41.33	32.99	−51.35	−9.621	−27.72
$B_s \to \pi^0 \pi^0$	—	—	∼0	—	—	−13.20	—	—	∼0	—	—	−13.85
$B_s \to \pi^0 \eta$	−19.61	−24.43	−24.23	−1.895	−47.90	−28.43	−20.90	−21.71	−23.25	−2.837	−48.02	−29.99
$B_s \to \pi^0 \eta'$	−19.61	−25.14	−24.59	−1.895	−56.44	−70.43	−20.90	−21.59	−19.95	−2.837	−55.64	−67.73
$B_s \to \eta \eta$	1.425	2.538	1.571	3.829	9.317	6.693	1.558	2.834	1.737	4.150	10.20	7.296
$B_s \to \eta \eta'$	−0.833	−0.627	−0.440	3.348	4.287	4.659	−0.909	−0.687	−0.482	3.628	4.655	5.063
$B_s \to \eta' \eta'$	−3.490	−2.196	−1.608	2.479	−0.553	0.414	−3.795	−2.360	−1.734	2.656	−0.605	0.441
$B_s \to K^{\pm} K^{\mp}$	−6.978	−7.101	−4.318	−42.09	−40.99	−27.24	−6.371	−6.512	−4.180	−41.84	−40.84	−27.83
$B_s \to \pi^{\pm} \pi^{\mp}$	—	—	∼0	—	—	−13.20	—	—	∼0	—	—	−13.85

puted with amplitudes $\mathcal{A}^f + \mathcal{A}^a$ and $\overline{\mathcal{A}^f + \mathcal{A}^a}$, including chirally enhanced hard spectator scattering contributions and annihilation effects. A number of observations are in order.

(i) From Tables VIII and IX, we can see that, as expected, as a result of the large parameter x_s suppression, the *CP*-violating asymmetry $\mathcal{A}_{CP}$ for those case-II decay modes is indeed very small, not exceeding 5%.

(ii) From the QCDF formula, Eq. (9), we know that ''nonfactorizable'' contributions are either at the order of α_s or power-suppressed in Λ_{QCD}/m_b, so the direct *CP*-violating asymmetries $\mathcal{A}_{CP}$ for those a_1 dominant decays, such as $B_s \to K^{(*)\pm} \pi^{\mp}, K^{\pm} \rho^{\mp}$, should not be large because of the small strong phases. The direct *CP*-violating asymmetries for pure annihilation B_s decays are near zero within the QCDF framework.

(iii) From previous $B \to PP, PV$ analysis [21,22] and Fig. 1, we know that ''nonfactorizable'' effects contribute a large imaginary part to the coefficients $a_{2,4,6}$; hence, there might be large direct *CP*-violating asymmetries for those $a_{2,4,6}$ dominant decays, such as $B_s \to K_S^0 \pi^0, K_S^0 \eta^{(\prime)}, \ldots$. In addition, the numbers in Table VII show that the *CP*-violating asymmetries of those decays are strongly affected by the contributions of chirally enhanced hard spectator scattering and annihilation interactions.

If we assume that the B_s^0-$\bar{B}_s^0$ mixing phase is negligible or $q/p \simeq 1$, it is possible to extract the weak angle γ or β from measurements of *CP*-violating asymmetries for B_s decays. Unfortunately, very rapid B_s^0-$\bar{B}_s^0$ oscillations are expected due to the large mixing parameter x_s, which makes experimental studies of the *CP* violation in the B_s meson system difficult, and only bounds on few decays modes are given for the moment. In addition, there exist large theoretical uncertainties. Within the QCDF approach, the subleading power corrections in $1/m_b$ might be as important as the radiative corrections numerically because m_b is large but finite. So the QCDF approach could only give the order of magnitude of the *CP*-violating asymmetries, as stated in [22].

TABLE VII. The *CP*-violating asymmetry parameters $a_{\epsilon'}$ and $a_{\epsilon+\epsilon'}$ for $B_s \to PV$ decays (in units of percent) with the QCDF approach; the captions are the same as in Table VI.

Modes	$a_{\epsilon'2}$	$a_{\epsilon'3}$	$a_{\epsilon'4}$	$a_{\epsilon+\epsilon'2}$	$a_{\epsilon+\epsilon'3}$	$a_{\epsilon+\epsilon'4}$	$a_{\epsilon'2}$	$a_{\epsilon'3}$	$a_{\epsilon'4}$	$a_{\epsilon+\epsilon'2}$	$a_{\epsilon+\epsilon'3}$	$a_{\epsilon+\epsilon'4}$
$B_s \to K_S^0 \rho^0$	−85.81	−18.34	−6.097	48.05	76.22	41.25	−91.47	−19.98	−5.602	3.010	15.43	−29.26
$B_s \to K_S^0 \omega$	93.12	23.61	13.61	32.48	96.95	94.80	100.0	31.47	19.56	0.563	74.83	97.05
$B_s \to K_S^0 \phi$	9.072	7.058	3.758	−77.48	−76.95	−75.15	7.383	5.760	3.092	−74.71	−74.20	−72.60
$B_s \to \pi^0 \rho^0$	—	—	∼0	—	—	72.86	—	—	∼0	—	—	85.30
$B_s \to \pi^0 \omega$	—	—	∼0	—	—	87.97	—	—	∼0	—	—	36.75
$B_s \to \pi^0 \phi$	−19.61	−24.49	—	−1.895	−48.52	—	−20.90	−21.71	—	−2.837	−48.57	—
$B_s \to \eta \rho^0$	−20.59	−25.52	−16.92	−2.143	−49.99	−30.87	−21.92	−22.48	−16.12	−3.183	−49.98	−31.79
$B_s \to \eta' \rho^0$	−20.59	−26.19	−32.96	−2.143	−58.68	−71.01	−21.92	−22.28	−26.55	−3.183	−57.70	−69.11
$B_s \to \eta \omega$	−71.80	3.677	0.762	11.57	98.69	83.42	−77.03	5.309	0.895	−0.750	94.91	26.73
$B_s \to \eta' \omega$	−71.80	6.333	4.356	11.57	96.02	91.76	−77.03	9.238	6.376	−0.750	98.53	99.69
$B_s \to \eta \phi$	6.180	42.45	23.24	2.003	−4.905	−18.26	6.705	44.21	23.21	2.084	−9.014	−19.98
$B_s \to \eta' \phi$	15.39	−10.95	−58.34	9.025	−28.48	−47.93	17.14	−10.54	−50.62	9.350	−29.20	−53.27

TABLE VIII. The *CP*-violating asymmetry parameters $\mathcal{A}_{CP}$ (%) for $B_s \to PP$ decays calculated with the QCDF approach, using the default input parameters. The numbers in columns 3–5 (see the text for their meanings) are computed with $A=0.824$, $\lambda=0.2236$, $\bar{\rho}=0.22$, $\bar{\eta}=0.35$, and $\gamma=59°$, while the numbers in columns 6–8 are computed with $A=0.82$, $\lambda=0.22$, $\bar{\rho}=0.086$, $\bar{\eta}=0.39$, and $\gamma=78.8°$.

Modes	Case	$\mathcal{A}_{CP2}$	$\mathcal{A}_{CP3}$	$\mathcal{A}_{CP4}$	$\mathcal{A}_{CP2}$	$\mathcal{A}_{CP3}$	$\mathcal{A}_{CP4}$
$B_s \to K^0 \bar{K}^0$	II	0.166	0.166	0.171	0.180	0.180	0.185
$B_s \to K_S^0 \pi^0$	II	−3.130	−0.517	−2.369	−3.502	−3.298	−4.219
$B_s \to K_S^0 \eta$	II	−1.808	2.270	1.173	−2.863	−1.128	−2.113
$B_s \to K_S^0 \eta'$	II	−2.077	−0.200	−1.129	−2.430	−0.377	−1.300
$B_s \to \pi^0 \pi^0$	II	—	—	−0.659	—	—	−0.691
$B_s \to \pi^0 \eta$	II	−0.143	−2.450	−1.478	−0.194	−2.449	−1.554
$B_s \to \pi^0 \eta'$	II	−0.143	−2.877	−3.574	−0.194	−2.829	−3.428
$B_s \to \eta \eta$	II	0.195	0.471	0.338	0.211	0.516	0.368
$B_s \to \eta \eta'$	II	0.165	0.212	0.231	0.179	0.230	0.251
$B_s \to \eta' \eta'$	II	0.115	−0.033	0.017	0.123	−0.036	0.018
$\bar{B}_s^0 \to K^+ \pi^-$	I	−4.267	−4.551	−5.863	−5.690	−6.081	−8.068
$B_s \to K^\pm K^\mp$	II	−2.117	−2.062	−1.369	−2.103	−2.053	−1.399
$B_s \to \pi^\pm \pi^\mp$	II	—	—	−0.659	—	—	−0.691

VI. EXTRACTING WEAK PHASES FROM $B_s \to KK$ DECAYS

It is important to test the self-consistency of the CKM description of *CP* violation through a variety of processes. One test involves the $B_d(t) \to \pi^+ \pi^-$ decays which are potentially rich sources of information of both strong and weak phases. Experimentally, BABAR and Belle have reported measurements of the *CP*-violating asymmetries in $B_d(t) \to \pi^+ \pi^-$ decays:

TABLE IX. The *CP*-violating asymmetry parameters $\mathcal{A}_{CP}$ (%) for $B_s \to PV$ decays; the captions are the same as in Table VIII.

Modes	Case	$\mathcal{A}_{CP2}$	$\mathcal{A}_{CP3}$	$\mathcal{A}_{CP4}$	$\mathcal{A}_{CP2}$	$\mathcal{A}_{CP3}$	$\mathcal{A}_{CP4}$
$B_s^0 \to K_S^0 \bar{K}^{*0}$	III	0.963	0.988	0.416	1.050	1.077	0.453
$B_s^0 \to K_S^0 K^{*0}$	III	−0.711	−0.688	−0.081	−0.776	−0.752	−0.090
$B_s^0 \to K^+ K^{*-}$	III	13.32	12.96	−14.34	12.96	13.12	−14.48
$B_s^0 \to K^- K^{*+}$	III	−14.06	−14.69	12.72	−11.52	−12.62	13.53
$B_s^0 \to \pi^+ \rho^-$	III	—	—	−3.634	—	—	−4.254
$B_s^0 \to \pi^- \rho^+$	III	—	—	−3.634	—	—	−4.254
$B_s^0 \to K_S^0 \rho^0$	II	2.182	3.756	2.042	−0.078	0.720	−1.473
$B_s^0 \to K_S^0 \omega$	II	1.852	4.894	4.762	0.277	3.811	4.889
$B_s^0 \to K_S^0 \phi$	II	−3.842	−3.820	−3.739	−3.708	−3.687	−3.613
$\bar{B}_s^0 \to \pi^0 K^{*0}$	I	−90.13	−21.55	−6.596	−99.16	−30.34	−9.403
$B_s \to \pi^0 \rho^0$	II	—	—	3.634	—	—	4.254
$B_s \to \pi^0 \omega$	II	—	—	4.387	—	—	1.833
$B_s \to \pi^0 \phi$	II	−0.143	−2.481	—	−0.194	−2.477	—
$\bar{B}_s^0 \to \eta K^{*0}$	I	48.35	49.06	3.703	39.99	37.04	2.546
$\bar{B}_s^0 \to \eta' K^{*0}$	I	−57.74	−32.24	−19.02	−73.64	−44.86	−25.30
$B_s \to \eta \rho^0$	II	−0.158	−2.557	−1.582	−0.213	−2.549	−1.626
$B_s \to \eta' \rho^0$	II	−0.158	−2.992	−3.624	−0.213	−2.933	−3.513
$B_s \to \eta \omega$	II	0.398	4.931	4.162	−0.23	4.747	1.335
$B_s \to \eta' \omega$	II	0.398	4.805	4.588	−0.23	4.937	4.988
$B_s \to \eta \phi$	II	0.115	−0.139	−0.853	0.121	−0.339	−0.938
$B_s \to \eta' \phi$	II	0.489	−1.448	−2.536	0.509	−1.483	−2.783
$\bar{B}_s^0 \to K^+ \rho^-$	I	−2.018	−2.164	3.552	−2.528	−2.706	4.572
$\bar{B}_s^0 \to \pi^- K^{*+}$	I	0.009	−0.031	−10.52	0.011	−0.036	−11.38

	BABAR [4]	Belle [7]
$S_{\pi\pi}$	$-0.02\pm0.34\pm0.05$	$1.23\pm0.41^{+0.07}_{-0.08}$
$C_{\pi\pi}$	$-0.30\pm0.25\pm0.04$	$-0.77\pm0.27\pm0.08$

which has triggered high theoretical interest. Theoretically, if we assume that the penguin amplitudes are zero for $B_d(t) \to \pi^+\pi^-$ decays, the weak angle α could be extracted from $S_{\pi\pi}=-\sin 2\alpha$. Unfortunately, this relation is strongly polluted by penguin effects:

$$S_{\pi\pi}=S_{\pi\pi}(\beta,\alpha,|P_{\pi\pi}/T_{\pi\pi}|,\delta_P-\delta_T),$$

$$C_{\pi\pi}=C_{\pi\pi}(\beta,\gamma,|P_{\pi\pi}/T_{\pi\pi}|,\delta_P-\delta_T),$$

where $|P_{\pi\pi}/T_{\pi\pi}|$ is the penguin-to-tree ratio and δ_T (δ_P) is the strong phase of the tree (penguin) amplitudes. Note that the CKM angle β has been well determined by BABAR and Belle; we now have two observables $S_{\pi\pi}, C_{\pi\pi}$ with three variables—weak angles α or γ (where $\alpha+\beta+\gamma=\pi$), difference of strong phase $\delta_P-\delta_T$, and ratio $|P_{\pi\pi}/T_{\pi\pi}|$. The nature of the penguin-to-tree ratio leads to some indeterminacy in determining the weak angles and strong phases. Hence, it is very interesting to investigate the ratio of penguin-to-tree amplitudes. Using the *U*-spin symmetry, we can get some additional information on the penguin-to-tree ratio $P_{\pi\pi}/T_{\pi\pi}$ of $B_d\to\pi^+\pi^-$ decays from its counterpart $B_s\to K^+K^-$ as a cross-check. To illustrate, we describe the expressions for the decay amplitudes of $B_s\to K^+K^-$ and $B_d\to\pi^+\pi^-$ as follows:

$$\mathcal{A}(\overline{B}^0\to\pi^+\pi^-)=|T_{\pi\pi}|e^{-i\delta_T}e^{-i\gamma}+|P_{\pi\pi}|e^{-i\delta_P}, \quad (46)$$

$$\mathcal{A}(\overline{B}_s^0\to K^+K^-)=|T_c|e^{-i\delta_T^c}e^{-i\gamma}-|P_c|e^{-i\delta_P^c}, \quad (47)$$

where $\delta^{(c)}_{T,P}$ denote strong phases. Using the SU(3) flavor symmetry, we have [60]

$$\frac{|T_{\pi\pi}|}{|T_c|}=\frac{|V_{ub}V_{ud}^*|}{|V_{ub}V_{us}^*|}=\frac{1-\lambda^2/2}{\lambda}, \quad \text{for} \quad \delta_T=\delta_T^c, \quad (48)$$

$$\frac{|P_{\pi\pi}|}{|P_c|}=\frac{|V_{cb}V_{cd}^*|}{|V_{cb}V_{cs}^*|}=\frac{\lambda}{1-\lambda^2/2}, \quad \text{for} \quad \delta_P=\delta_P^c, \quad (49)$$

$$\frac{|P_{\pi\pi}|}{|T_{\pi\pi}|}=\tan^2\theta_c\frac{|P_c|}{|T_c|}, \quad \text{for} \quad \delta_T-\delta_P=\delta_T^c-\delta_P^c=\delta', \quad (50)$$

where θ_c is the Cabibbo angle and, with $r_A=f_{B_s}f_K/(F^{B_s\to K}m_{B_s}^2)$,

$$\frac{P_c}{T_c}=\frac{-|V_{cb}V_{cs}^*|\left\{a_4^c+a_{10}^c+r_\chi(a_6^c+a_8^c)+r_A\left(b_3+2b_4-\frac{1}{2}b_3^{ew}+\frac{1}{2}b_4^{ew}\right)\right\}}{|V_{ub}V_{us}^*|\left\{a_1^u+a_4^u+a_{10}^u+r_\chi(a_6^u+a_8^u)+r_A\left(b_1+b_3+2b_4-\frac{1}{2}b_3^{ew}+\frac{1}{2}b_4^{ew}\right)\right\}}. \quad (51)$$

Compared with $B_d\to\pi^+\pi^-$ decay, the contribution of T_c (P_c) for $B_s\to K^+K^-$ decay is reduced (enhanced) by $\tan\theta_c$. Of course, the relations of Eqs. (48) and (49) are affected by U-spin breaking effects, such as the factor $[(m_{B_d}^2-m_\pi^2)F^{B\to\pi}f_\pi]/[(m_{B_s}^2-m_K^2)F^{B_s\to K}f_K]$, and so on. But SU(3) flavor breaking effects are expected to be very small in Eq. (50) within the factorization approach. As stated in [61,62], assuming that the B_s^0-$\overline{B}_s^0$ mixing phase is negligible and taking the angle β as one known input which can be determined from $B_d\to J/\Psi K_S$ decays and has been tentatively given by BABAR [63] and Belle [64], the strong phase $\delta_T-\delta_P$ and $|P_{\pi\pi}/T_{\pi\pi}|$ (or $\delta_T^c-\delta_P^c$ and $|P_c/T_c|$) as a function of weak angle γ or/and α can be determined from measurements of $S_{\pi\pi}$ and $C_{\pi\pi}$ (or S_{KK} and C_{KK}). And employing Eq. (50) within the U-spin symmetry, the penguin-to-tree ratio can be overconstrained from $B_d\to\pi^+\pi^-$ and $B_s\to K^+K^-$ decays. And using the value of the penguin-to-tree ratios, some information on weak phases γ and/or α can be extracted from the measurements:

$$\lambda_{\pi\pi}=\frac{V_{td}V_{tb}^*}{V_{td}^*V_{tb}}\frac{\mathcal{A}(\overline{B}^0(0)\to\pi^+\pi^-)}{\mathcal{A}(B^0(0)\to\pi^+\pi^-)}=e^{i2\alpha}\frac{1+|P_{\pi\pi}/T_{\pi\pi}|e^{i\delta'}e^{i\gamma}}{1+|P_{\pi\pi}/T_{\pi\pi}|e^{i\delta'}e^{-i\gamma}}, \quad (52)$$

$$S_{\pi\pi}=\frac{-2\,\mathrm{Im}(\lambda_{\pi\pi})}{1+|\lambda_{\pi\pi}|^2}=\frac{-\sin 2\alpha+2|P_{\pi\pi}/T_{\pi\pi}|\cos\delta'\cos(\alpha-\beta)+|P_{\pi\pi}/T_{\pi\pi}|^2\sin 2\beta}{1-2|P_{\pi\pi}/T_{\pi\pi}|\cos\delta'\cos(\alpha+\beta)+|P_{\pi\pi}/T_{\pi\pi}|^2}, \quad (53)$$

TABLE X. Penguin-to-tree ratios and bound on γ, using the default input parameters, within the QCDF approach. The numbers in columns (see the text for their meanings) 3–5,9–11 are computed with $A=0.824$, $\lambda=0.2236$, $\bar{\rho}=0.22$, $\bar{\eta}=0.35$, and $\gamma=59°$, while the numbers in columns 6–8,12–14 are computed with $A=0.82$, $\lambda=0.22$, $\bar{\rho}=0.086$, $\bar{\eta}=0.39$, and $\gamma=78.8°$. The numbers in columns 3–8 are computed with asymptotic twist-2 and twist-3 light cone distribution amplitudes of K mesons, while the numbers in columns 9–14 are computed with twist-2 (including effects of Gegenbauer moments) and asymptotic twist-3 light cone distribution amplitudes of K mesons. The constraints on γ are calculated from $\cos\gamma \gtrsim (|P_c/T_c|)(1-\sqrt{R_{KK}})$.

		$\Phi_K(x)=6x\bar{x}, \Phi_K^p(x)=1,\ \Phi_K^\sigma(x)=6x\bar{x}$						$\Phi_K^p(x)=1, \quad \Phi_K^\sigma(x)=6x\bar{x},$ $\Phi_K(x)=6x\bar{x}\left[1+\sum_{n=1}^{2}\alpha_n^K C_n^{(3/2)}(2x-1)\right]$					
	λ_B (MeV)	N2	N3	N4	N2	N3	N4	N2	N3	N4	N2	N3	N4
$\lvert P_c/T_c\rvert$	200	4.305	4.502	6.753	4.610	4.821	7.233	4.133	4.470	6.965	4.427	4.788	7.460
	350	4.305	4.411	6.547	4.610	4.725	7.012	4.133	4.307	6.565	4.427	4.613	7.031
	500	4.305	4.378	6.471	4.610	4.689	6.930	4.133	4.250	6.425	4.427	4.552	6.882
$\lvert P_{\pi\pi}/T_{\pi\pi}\rvert$	200	0.226	0.237	0.355	0.234	0.245	0.368	0.217	0.235	0.366	0.225	0.243	0.379
	350	0.226	0.232	0.344	0.234	0.240	0.356	0.217	0.227	0.345	0.225	0.234	0.357
	500	0.226	0.230	0.340	0.234	0.238	0.352	0.217	0.224	0.338	0.225	0.231	0.350
δ'	200	8.254°	8.971°	8.501°	8.254°	8.971°	8.501°	6.861°	8.012°	7.780°	6.861°	8.012°	7.780°
	350	8.254°	8.649°	8.280°	8.254°	8.649°	8.280°	6.861°	7.474°	7.415°	6.861°	7.474°	7.415°
	500	8.254°	8.526°	8.195°	8.254°	8.526°	8.195°	6.861°	7.278°	7.279°	6.861°	7.278°	7.279°
R_{KK}	200	0.805	0.818	0.861	0.962	0.970	0.967	0.796	0.821	0.866	0.959	0.975	0.970
	350	0.805	0.812	0.855	0.962	0.967	0.965	0.796	0.809	0.855	0.959	0.968	0.965
	500	0.805	0.810	0.853	0.962	0.965	0.963	0.796	0.805	0.852	0.959	0.965	0.963
$\gamma\lesssim$	200	63.73°	64.58°	60.84°	84.94°	85.89°	83.19°	63.56°	65.12°	61.07°	84.78°	86.54°	83.60°
	350	63.73°	64.18°	60.52°	84.94°	85.45°	82.80°	63.56°	64.35°	60.46°	84.78°	85.67°	82.83°
	500	63.73°	64.04°	60.41°	84.94°	85.29°	82.66°	63.56°	64.09°	60.26°	84.78°	85.38°	82.57°

$$C_{\pi\pi}=\frac{1-|\lambda_{\pi\pi}|^2}{1+|\lambda_{\pi\pi}|^2}=\frac{2|P_{\pi\pi}/T_{\pi\pi}|\sin\delta'\sin\gamma}{1+2|P_{\pi\pi}/T_{\pi\pi}|\cos\delta'\cos\gamma+|P_{\pi\pi}/T_{\pi\pi}|^2}, \tag{54}$$

$$\lambda_{KK}=\frac{V_{ts}V_{tb}^*}{V_{ts}^*V_{tb}}\frac{\mathcal{A}(\bar{B}_s^0(0)\to K^+K^-)}{\mathcal{A}(B_s^0(0)\to K^+K^-)}=e^{-i2\gamma}\frac{1-|P_c/T_c|e^{i\delta'}e^{i\gamma}}{1-|P_c/T_c|e^{i\delta'}e^{-i\gamma}}, \tag{55}$$

$$S_{KK}=\frac{-2\,\mathrm{Im}(\lambda_{KK})}{1+|\lambda_{KK}|^2}=\frac{\sin 2\gamma-2|P_c/T_c|\cos\delta'\sin\gamma}{1-2|P_c/T_c|\cos\delta'\cos\gamma+|P_c/T_c|^2}, \tag{56}$$

$$C_{KK}=\frac{1-|\lambda_{KK}|^2}{1+|\lambda_{KK}|^2}=\frac{-2|P_c/T_c|\sin\delta'\sin\gamma}{1-2|P_c/T_c|\cos\delta'\cos\gamma+|P_c/T_c|^2}. \tag{57}$$

Here the numerical values of penguin-to-tree ratios within the QCDF approach are given in Table X. The numbers in the $N2$ columns are computed with amplitudes $\mathcal{A}^f$, but without contributions from hard spectator scattering interactions and annihilation topologies: i.e., coefficients $a_i=a_{i,I}$, $a_{i,II}=b_i=0$. The numbers in the $N3$ columns are computed with amplitudes $\mathcal{A}^f$, including chirally enhanced hard spectator scattering contributions, but without considering annihilation effects: i.e., $a_i=a_{i,I}+a_{i,II}$, $b_i=0$. The numbers in the $N4$ columns are computed with amplitudes $\mathcal{A}^f+\mathcal{A}^a$, including chirally enhanced hard spectator scattering contributions and annihilation effects. Although using different derivation and inputs, our results of the penguin-to-tree ratio $|P_{\pi\pi}/T_{\pi\pi}|$ using Eq. (50) are virtually in agreement with the result of $(28.5\pm5.1\mp5.7)\%$ (including weak annihilation contributions) and $(25.9\pm4.3\mp5.2)\%$ (without weak annihilation

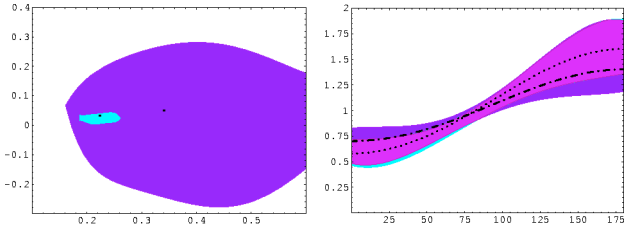

FIG. 6. Penguin-to-tree ratio $\mathrm{Im}(P_{\pi\pi}/T_{\pi\pi})$ (vertical axes) and $\mathrm{Re}(P_{\pi\pi}/T_{\pi\pi})$ (horizontal axes) of decay $B_d \to \pi^{\pm}\pi^{\mp}$ in (a), where the left and right dots denote the default result with and without the contributions of chirally enhanced hard spectator scattering and annihilation interactions, and R_{KK} versus the CKM angle γ in (b). The legends are the same as in Fig. 2(h).

contributions) [20] which is calculated with $X_A = X_H = \ln(m_B/\Lambda_h)$, and the result of $(27.6 \pm 6.4)\%$ [65] [including SU(3) breaking effects]. In addition, the value of the strong phase δ' is also consistent with $(8.2 \pm 3.8)°$ (including weak annihilation contributions) and $(9.0 \pm 4.1)°$ (without weak annihilation contributions) [20]. The numbers in Table X show that the parameters $(\lambda_B, \alpha_{1,2}^K)$ related to distribution amplitudes have a small influence upon the penguin-to-tree ratio, and Fig. 6(a) indicates $\delta' \in (1.3°, 10.0°)$ (without the contributions of chirally enhanced hard spectator scattering and annihilation interactions) and $\delta' \in (-38.5°, 42.8°)$ (including the contributions of chirally enhanced hard spectator scattering and annihilation interactions).

In addition, if the penguin-to-tree ratios are determined, then it is possible to extract some information or give a bound on the weak angle γ from the measurements of $B_s \to K^+K^-, \bar{K}^0K^0$ decays in the future. Now let us illustrate this point. The QCD penguin terms for these two decays should be equal according to factorization, so the decay amplitude for $B_s \to \bar{K}^0K^0$ could be written as

$$\mathcal{A}(\bar{B}_s^0 \to \bar{K}^0K^0) \simeq -|P_c| e^{-i\delta_P^c}. \tag{58}$$

There are two approximations in Eq. (58), as stated in [60]: (1) The color-suppressed terms which are proportional to the CKM matrix factor $V_{ub}V_{us}^*$ in Eqs. (A1) and (C1) can be safely neglected because of $|V_{ub}V_{us}^*/V_{cb}V_{cs}^*| \simeq 2\%$. (2) The tiny isospin breaking effects are disregarded, and the small difference of electroweak penguin contributions between these two decay modes are neglected. The ratio of *CP*-averaged branching ratios is defined as

$$R_{KK} = \frac{BR(\bar{B}_s^0 \to K^+K^-) + BR(B_s^0 \to K^+K^-)}{BR(\bar{B}_s^0 \to \bar{K}^0K^0) + BR(B_s^0 \to \bar{K}^0K^0)}$$

$$= \frac{1 - 2|P_c/T_c|\cos\delta'\cos\gamma + |P_c/T_c|^2}{|P_c/T_c|^2}. \tag{59}$$

Then we can get a constraint on γ:

$$\cos\gamma \gtrsim \left|\frac{P_c}{T_c}\right|(1 - \sqrt{R_{KK}}). \tag{60}$$

In addition, Gronau and Ronsner also gave a bound on γ from the decays $B_s \to K^+K^-, \bar{K}^0K^0$ without prior knowledge of the penguin-to-tree ratio, $\sin^2\gamma \leqslant R_{KK}$ [60].

From the above discussion, we can see that precise measurements of B_s decays in the future might resolve ambiguities in the determination of the CKM angles. In addition, the theoretical uncertainty is small in Fig. 6(b) because many unknown hadronic quantities are canceled with the ratio R_{KK}, and the results in Table X indicate that the weak angle γ given in Refs. [34,45] and the bound from Eq. (60) are consistent with each other, which might be tested in future measurements.

VII. SUMMARY AND CONCLUSION

In this paper, we calculated the *CP*-averaged branching ratios and *CP*-violating asymmetries of two-body charmless hadronic $B_s \to PP, PV$ decays at next-to-leading order in α_s with the QCDF approach, including chirally enhanced power corrections, as well as contributions from weak annihilation topologies. We find the following.

Only several decays, such as $B_s \to K^{(*)}K, K^{(*)\pm}\pi^{\mp}$, $K^{\pm}\rho^{\mp}, \eta^{(\prime)}\eta^{(\prime)}$, have large branching ratios, which might be accessible at hadron colliders in the near future.

For a_1 dominant decays, such as $B_s \to K^{(*)\pm}\pi^{\mp}, K^{\pm}\rho^{\mp}$, the hard radiative corrections are small, which results in small strong phases and small direct *CP*-violating asymmetries. In addition, for these decay modes, the predictions of the QCDF approach of *CP*-averaged branching ratios have only small differences with those of the NF scheme.

Large direct *CP*-violating asymmetries occur in some decay modes whose decay amplitudes are related to $a_{2,4,6}$ which obtain a large imaginary part from "nonfactorizable" effects. But time-integrated $\mathcal{A}_{CP}$ for case-II *CP* decays is always small because of the suppression from the large parameter x_s. In addition, the contribution of power corrections in $1/m_b$ [which are neglected in the QCDF formula, Eq. (9)] to the strong phase might be as important as hard radiative corrections, so the numerical results of *CP*-violating asymmetries of B_s decays with the QCDF approach should not be taken too seriously.

The penguin-to-tree ratio $|P_{\pi\pi}/T_{\pi\pi}|$ of $B_d \to \pi^+\pi^-$ decays can be overconstrained from its SU(3) counterpart $B_s \to K^+K^-$ using the U-spin symmetry, and a bound on the CKM angle γ can be obtained from $B_s \to K^+K^-, K^0\bar{K}^0$ decays. We look forward to future measurements and theoretical developments to give some insight into these parameters.

ACKNOWLEDGMENTS

This work is supported in part by National Natural Science Foundation of China. G.Z. thanks JSPS of Japan for financial support.

APPENDIX A: THE DECAY AMPLITUDES FOR $\bar{B}_s^0 \to PP$

$$\mathcal{A}^f(\bar{B}_s^0 \to K^0 \bar{K}^0) = -i\frac{G_F}{\sqrt{2}} f_K F_0^{B_s^0 \to K}(m_{B_s}^2 - m_K^2)(V_{ub}V_{us}^* + V_{cb}V_{cs}^*)\left\{ a_4 - \frac{1}{2}a_{10} + R_1\left(a_6 - \frac{1}{2}a_8 \right) \right\}, \tag{A1}$$

where $R_1 = 2m_{K^0}^2/(m_s + m_d)(m_b - m_d)$;

$$\mathcal{A}^f(\bar{B}_s^0 \to K^0 \pi^0) = -i\frac{G_F}{2} f_\pi F_0^{B_s^0 \to K}(m_{B_s}^2 - m_K^2)\left\{ V_{ub}V_{ud}^* a_2 + (V_{ub}V_{ud}^* + V_{cb}V_{cd}^*)\left[-a_4 + \frac{1}{2}a_{10} - \frac{3}{2}(a_7 - a_9) - R_2 \right.\right.$$
$$\left.\left. \times\left(a_6 - \frac{1}{2}a_8 \right) \right] \right\}, \tag{A2}$$

where $R_2 = 2m_{\pi^0}^2/(m_u + m_d)(m_b - m_d)$;

$$\mathcal{A}^f(\bar{B}_s^0 \to K^0 \eta^{(\prime)}) = -i\frac{G_F}{\sqrt{2}} f_K F_0^{B_s^0 \to \eta^{(\prime)}}(m_{B_s}^2 - m_{\eta^{(\prime)}}^2)(V_{ub}V_{ud}^* + V_{cb}V_{cd}^*)\left\{ a_4 - \frac{1}{2}a_{10} + R_3\left(a_6 - \frac{1}{2}a_8 \right) \right\}$$
$$-i\frac{G_F}{\sqrt{2}} f_{\eta^{(\prime)}}^u F_0^{B_s^0 \to K}(m_{B_s}^2 - m_K^2)\left\{ V_{ub}V_{ud}^* a_2 + (V_{ub}V_{ud}^* + V_{cb}V_{cd}^*)\left[2(a_3 - a_5) + a_4 - \frac{1}{2}a_{10} - \frac{1}{2}(a_7 - a_9) \right.\right.$$
$$\left.\left. + R_4^{(\prime)}\left(a_6 - \frac{1}{2}a_8 \right)\left(1 - \frac{f_{\eta^{(\prime)}}^u}{f_{\eta^{(\prime)}}^s} \right) + \left(a_3 - a_5 + \frac{1}{2}a_7 - \frac{1}{2}a_9 \right)\frac{f_{\eta^{(\prime)}}^s}{f_{\eta^{(\prime)}}^u} \right] \right\}, \tag{A3}$$

where $R_3 = 2m_{K^0}^2/(m_s + m_d)(m_b - m_s)$ and $R_4^{(\prime)} = 2m_{\eta^{(\prime)}}^2/(m_s + m_s)(m_b - m_d)$;

$$\mathcal{A}^f(\bar{B}_s^0 \to \pi^0 \eta^{(\prime)}) = -i\frac{G_F}{2} f_\pi F_0^{B_s^0 \to \eta^{(\prime)}}(m_{B_s}^2 - m_{\eta^{(\prime)}}^2)\left\{ V_{ub}V_{us}^* a_2 + (V_{ub}V_{us}^* + V_{cb}V_{cs}^*)\left[-\frac{3}{2}(a_7 - a_9) \right] \right\}, \tag{A4}$$

$$\mathcal{A}^f(\bar{B}_s^0 \to \eta^{(\prime)} \eta^{(\prime)}) = -i\sqrt{2} G_F f_{\eta^{(\prime)}}^u F_0^{B_s^0 \to \eta^{(\prime)}}(m_{B_s}^2 - m_{\eta^{(\prime)}}^2)\left\{ V_{ub}V_{us}^* a_2 + (V_{ub}V_{us}^* + V_{cb}V_{cs}^*) \right.$$
$$\times\left[2(a_3 - a_5) - \frac{1}{2}(a_7 - a_9) \right] + (V_{ub}V_{us}^* + V_{cb}V_{cs}^*)\frac{f_{\eta^{(\prime)}}^s}{f_{\eta^{(\prime)}}^u}\left[a_3 - a_5 + a_4 - \frac{1}{2}a_{10} + \frac{1}{2}a_7 - \frac{1}{2}a_9 \right.$$
$$\left.\left. + R_5^{(\prime)}\left(a_6 - \frac{1}{2}a_8 \right)\left(1 - \frac{f_{\eta^{(\prime)}}^u}{f_{\eta^{(\prime)}}^s} \right) \right] \right\}, \tag{A5}$$

where $R_5^{(\prime)} = 2m_{\eta^{(\prime)}}^2/(m_s + m_s)(m_b - m_s)$;

$$\mathcal{A}^f(\bar{B}_s^0 \to \eta\eta') = -i\frac{G_F}{\sqrt{2}} f_\eta^u F_0^{B_s^0 \to \eta'}(m_{B_s}^2 - m_{\eta'}^2)\left\{ V_{ub}V_{us}^* a_2 + (V_{ub}V_{us}^* + V_{cb}V_{cs}^*)\left[2(a_3 - a_5) - \frac{1}{2}(a_7 - a_9) \right] \right.$$
$$+ (V_{ub}V_{us}^* + V_{cb}V_{cs}^*)\frac{f_\eta^s}{f_\eta^u}\left[a_3 - a_5 + a_4 - \frac{1}{2}a_{10} + \frac{1}{2}a_7 - \frac{1}{2}a_9 + R_5\left(a_6 - \frac{1}{2}a_8 \right)\left(1 - \frac{f_\eta^u}{f_\eta^s} \right) \right] \Big\} - i\frac{G_F}{\sqrt{2}} f_{\eta'}^u F_0^{B_s^0 \to \eta}$$
$$\times(m_{B_s}^2 - m_\eta^2)\left\{ V_{ub}V_{us}^* a_2 + (V_{ub}V_{us}^* + V_{cb}V_{cs}^*)\left[2(a_3 - a_5) - \frac{1}{2}(a_7 - a_9) \right] + (V_{ub}V_{us}^* + V_{cb}V_{cs}^*)\frac{f_{\eta'}^s}{f_{\eta'}^u} \right.$$
$$\left.\times\left[a_3 - a_5 + a_4 - \frac{1}{2}a_{10} + \frac{1}{2}a_7 - \frac{1}{2}a_9 + R_5'\left(a_6 - \frac{1}{2}a_8 \right)\left(1 - \frac{f_{\eta'}^u}{f_{\eta'}^s} \right) \right] \right\}, \tag{A6}$$

$$\mathcal{A}^f(\overline{B}_s^0\to\pi^-K^+)=-i\frac{G_F}{\sqrt{2}}f_\pi F_0^{B_s^0\to K}(m_{B_s}^2-m_K^2)\{V_{ub}V_{ud}^*\alpha_1+(V_{ub}V_{ud}^*+V_{cb}V_{cd}^*)[a_4+a_{10}+R_6(a_6+a_8)]\},\tag{A7}$$

where $R_6=2m_{\pi^+}^2/(m_u+m_d)(m_b-m_u)$;

$$\mathcal{A}^f(\overline{B}_s^0\to K^-K^+)=-i\frac{G_F}{\sqrt{2}}f_K F_0^{B_s^0\to K}(m_{B_s}^2-m_K^2)\{V_{ub}V_{us}^*a_1+(V_{ub}V_{us}^*+V_{cb}V_{cs}^*)[a_4+a_{10}+R_7(a_6+a_8)]\},\tag{A8}$$

where $R_7=2m_{K^-}^2/(m_u+m_s)(m_b-m_u)$.

APPENDIX B: THE DECAY AMPLITUDES FOR $\overline{B}_s^0\to PV$

$$\mathcal{A}^f(\overline{B}_s^0\to K^0\overline{K}^{*0})=\sqrt{2}G_F f_{K^*}F_1^{B_s^0\to K}m_{K^*}(\epsilon\cdot p_{K^0})(V_{ub}V_{us}^*+V_{cb}V_{cs}^*)\left\{a_4-\frac{1}{2}a_{10}\right\},\tag{B1}$$

$$\mathcal{A}^f(\overline{B}_s^0\to\overline{K}^0K^{*0})=\sqrt{2}G_F f_K A_0^{B_s^0\to K^*}m_{K^*}(\epsilon\cdot p_{\overline{K}^0})(V_{ub}V_{us}^*+V_{cb}V_{cs}^*)\left\{a_4-\frac{1}{2}a_{10}-Q_1\left(a_6-\frac{1}{2}a_8\right)\right\},\tag{B2}$$

where $Q_1=2m_{\overline{K}^0}^2/(m_s+m_d)(m_b+m_d)$;

$$\mathcal{A}^f(\overline{B}_s^0\to K^0\rho^0)=G_F f_\rho F_1^{B_s^0\to K}m_\rho(\epsilon\cdot p_{K^0})\left\{V_{ub}V_{ud}^*a_2+(V_{ub}V_{ud}^*+V_{cb}V_{cd}^*)\left[-a_4+\frac{1}{2}a_{10}+\frac{3}{2}a_7+\frac{3}{2}a_9\right]\right\},\tag{B3}$$

$$\begin{aligned}\mathcal{A}^f(\overline{B}_s^0\to K^0\omega)=G_F f_\omega F_1^{B_s^0\to K}m_\omega(\epsilon\cdot p_{K^0})&\left\{V_{ub}V_{ud}^*a_2+(V_{ub}V_{ud}^*+V_{cb}V_{cd}^*)\right.\\&\left.\times\left[2(a_3+a_5)+a_4-\frac{1}{2}a_{10}+\frac{1}{2}a_7+\frac{1}{2}a_9\right]\right\},\end{aligned}\tag{B4}$$

$$\begin{aligned}\mathcal{A}^f(\overline{B}_s^0\to K^0\phi)=\sqrt{2}G_F m_\phi(\epsilon\cdot p_{K^0})&(V_{ub}V_{ud}^*+V_{cb}V_{cd}^*)\\&\times\left\{f_\phi F_1^{B_s^0\to K}\left[a_3+a_5-\frac{1}{2}a_7-\frac{1}{2}a_9\right]+f_K A_0^{B_s^0\to\phi}\left[a_4-\frac{1}{2}a_{10}-Q_2\left(a_6-\frac{1}{2}a_8\right)\right]\right\},\end{aligned}\tag{B5}$$

where $Q_2=2m_{K^0}^2/(m_s+m_d)(m_b+m_s)$;

$$\begin{aligned}\mathcal{A}^f(\overline{B}_s^0\to\pi^0K^{*0})=G_F f_\pi A_0^{B_s^0\to K^{*0}}m_{K^{*0}}(\epsilon\cdot p_{\pi^0})&\left\{V_{ub}V_{ud}^*a_2+(V_{ub}V_{ud}^*+V_{cb}V_{cd}^*)\left[-a_4+\frac{1}{2}a_{10}-\frac{3}{2}a_7+\frac{3}{2}a_9\right.\right.\\&\left.\left.+Q_3\left(a_6-\frac{1}{2}a_8\right)\right]\right\},\end{aligned}\tag{B6}$$

where $Q_3=2m_{\pi^0}^2/(m_u+m_d)(m_b+m_d)$;

$$\mathcal{A}^f(\overline{B}_s^0\to\pi^0\phi)=G_F f_\pi A_0^{B_s^0\to\phi}m_\phi(\epsilon\cdot p_{\pi^0})\left\{V_{ub}V_{us}^*a_2+(V_{ub}V_{us}^*+V_{cb}V_{cs}^*)\left[-\frac{3}{2}a_7+\frac{3}{2}a_9\right]\right\},\tag{B7}$$

$$\mathcal{A}^f(\bar{B}_s^0\to\eta^{(\prime)}K^{*0})=\sqrt{2}G_F m_{K^{*0}}(\epsilon\cdot p_{\eta^{(\prime)}})\Bigg(f^u_{\eta^{(\prime)}}A_0^{B_s^0\to K^{*0}}\Bigg\{V_{ub}V_{ud}^*a_2+(V_{ub}V_{ud}^*+V_{cb}V_{cd}^*)\Bigg[2(a_3-a_5)+a_4-\frac{1}{2}a_{10}-\frac{1}{2}a_7$$
$$+\frac{1}{2}a_9-Q_4^{(\prime)}\Big(a_6-\frac{1}{2}a_8\Big)\Big(1-\frac{f^u_{\eta^{(\prime)}}}{f^s_{\eta^{(\prime)}}}\Big)\Bigg]+(V_{ub}V_{ud}^*+V_{cb}V_{cd}^*)\frac{f^s_{\eta^{(\prime)}}}{f^u_{\eta^{(\prime)}}}$$
$$\times\Big(a_3-a_5+\frac{1}{2}a_7-\frac{1}{2}a_9\Big)\Bigg\}+f_{K*}F_1^{B_s^0\to\eta^{(\prime)}}(V_{ub}V_{ud}^*+V_{cb}V_{cd}^*)\Big(a_4-\frac{1}{2}a_{10}\Big)\Bigg),\tag{B8}$$

where $Q_4^{(\prime)}=2m^2_{\eta^{(\prime)}}/(m_s+m_s)(m_b+m_s)$;

$$\mathcal{A}^f(\bar{B}_s^0\to\eta^{(\prime)}\rho^0)=G_F f_\rho F_1^{B_s^0\to\eta^{(\prime)}}m_\rho(\epsilon\cdot p_{\eta^{(\prime)}})\Big\{V_{ub}V_{us}^*a_2+(V_{ub}V_{us}^*+V_{cb}V_{cs}^*)\Big[\frac{3}{2}(a_7+a_9)\Big]\Big\},\tag{B9}$$

$$\mathcal{A}^f(\bar{B}_s^0\to\eta^{(\prime)}\omega)=G_F f_\omega F_1^{B_s^0\to\eta^{(\prime)}}m_\omega(\epsilon\cdot p_{\eta^{(\prime)}})\Big\{V_{ub}V_{us}^*a_2+(V_{ub}V_{us}^*+V_{cb}V_{cs}^*)\Big[2(a_3+a_5)+\frac{1}{2}(a_7+a_9)\Big]\Big\},\tag{B10}$$

$$\mathcal{A}^f(\bar{B}_s^0\to\eta^{(\prime)}\phi)=\sqrt{2}G_F m_\phi(\epsilon\cdot p_{\eta^{(\prime)}})\Bigg(f^u_{\eta^{(\prime)}}A_0^{B_s^0\to\phi}\Bigg\{V_{ub}V_{us}^*a_2+(V_{ub}V_{us}^*+V_{cb}V_{cs}^*)\Big(2(a_3-a_5)$$
$$-\frac{1}{2}(a_7-a_9)\Big)+(V_{ub}V_{us}^*+V_{cb}V_{cs}^*)\frac{f^s_{\eta^{(\prime)}}}{f^u_{\eta^{(\prime)}}}\Bigg[a_3-a_5+a_4-\frac{1}{2}a_{10}+\frac{1}{2}a_7-\frac{1}{2}a_9-Q_4^{(\prime)}\Big(a_6-\frac{1}{2}a_8\Big)$$
$$\times\Big(1-\frac{f^u_{\eta^{(\prime)}}}{f^s_{\eta^{(\prime)}}}\Big)\Bigg]\Bigg\}+f_\phi F_1^{B_s^0\to\eta^{(\prime)}}(V_{ub}V_{us}^*+V_{cb}V_{cs}^*)\Big(a_3+a_5+a_4-\frac{1}{2}a_{10}-\frac{1}{2}a_7-\frac{1}{2}a_9\Big)\Bigg),\tag{B11}$$

$$\mathcal{A}^f(\bar{B}_s^0\to K^+\rho^-)=\sqrt{2}G_F f_\rho F_1^{B_s^0\to K}m_\rho(\epsilon\cdot p_K)\{V_{ub}V_{ud}^*a_1+(V_{ub}V_{ud}^*+V_{cb}V_{cd}^*)(a_4+a_{10})\},\tag{B12}$$

$$\mathcal{A}^f(\bar{B}_s^0\to K^+K^{*-})=\sqrt{2}G_F f_{K*}F_1^{B_s^0\to K}m_{K*}(\epsilon\cdot p_K)\{V_{ub}V_{us}^*a_1+(V_{ub}V_{us}^*+V_{cb}V_{cs}^*)(a_4+a_{10})\},\tag{B13}$$

$$\mathcal{A}^f(\bar{B}_s^0\to K^-K^{*+})=\sqrt{2}G_F f_K A_0^{B_s^0\to K^*}m_{K*}(\epsilon\cdot p_K)\{V_{ub}V_{us}^*a_1+(V_{ub}V_{us}^*+V_{cb}V_{cs}^*)[a_4+a_{10}-Q_5(a_6+a_8)]\},\tag{B14}$$

where $Q_5=2m^2_{K^-}/(m_u+m_s)(m_b+m_u)$;

$$\mathcal{A}^f(\bar{B}_s^0\to\pi^-K^{*+})=\sqrt{2}G_F f_\pi A_0^{B_s^0\to K^*}m_{K*}(\epsilon\cdot p_\pi)\{V_{ub}V_{ud}^*a_1+(V_{ub}V_{ud}^*+V_{cb}V_{cd}^*)[a_4+a_{10}-Q_6(a_6+a_8)]\},\tag{B15}$$

where $Q_6=2m^2_{\pi^-}/(m_u+m_d)(m_b+m_u)$.

APPENDIX C: THE WEAK ANNIHILATION AMPLITUDES FOR $\bar{B}_s^0\to PP$

$$\mathcal{A}^a(\bar{B}_s^0\to K^0\bar{K}^0)=-i\frac{G_F}{\sqrt{2}}f_{B_s}f_K^2\Bigg\{(V_{ub}V_{us}^*+V_{cb}V_{cs}^*)\Bigg[b_3(\bar{K}^0,K^0)+b_4(\bar{K}^0,K^0)+b_4(K^0,\bar{K}^0)-\frac{1}{2}b_3^{ew}(\bar{K}^0,K^0)-\frac{1}{2}b_4^{ew}(\bar{K}^0,K^0)$$
$$-\frac{1}{2}b_4^{ew}(K^0,\bar{K}^0)\Bigg]\Bigg\},\tag{C1}$$

$$\mathcal{A}^a(\bar{B}_s^0\to K^0\pi^0)=i\frac{G_F}{2}f_{B_s}f_K f_\pi(V_{ub}V_{ud}^*+V_{cb}V_{cd}^*)\Big\{b_3(\pi^0,K^0)-\frac{1}{2}b_3^{ew}(\pi^0,K^0)\Big\},\tag{C2}$$

$$\mathcal{A}^a(\bar{B}_s^0\to K^0\eta^{(\prime)})=-i\frac{G_F}{\sqrt{2}}f_{B_s}f_K(V_{ub}V_{ud}^*+V_{cb}V_{cd}^*)\Big\{f^u_{\eta^{(\prime)}}\Big[b_3(\eta^{(\prime)},K^0)-\frac{1}{2}b_3^{ew}(\eta^{(\prime)},K^0)\Big]+f^s_{\eta^{(\prime)}}\times\Big[b_3(K^0,\eta^{(\prime)})-\frac{1}{2}b_3^{ew}(K^0,\eta^{(\prime)})\Big]\Big\},\tag{C3}$$

$$\mathcal{A}^a(\bar{B}_s^0\to\pi^0\pi^0)=-i\frac{G_F}{\sqrt{2}}f_{B_s}f_\pi^2\Big\{V_{ub}V_{us}^*b_1(\pi^0,\pi^0)+(V_{ub}V_{us}^*+V_{cb}V_{cs}^*)\Big[2b_4(\pi^0,\pi^0)+\frac{1}{2}b_4^{ew}(\pi^0,\pi^0)\Big]\Big\},\tag{C4}$$

$$\mathcal{A}^a(\bar{B}_s^0\to\pi^0\eta^{(\prime)})=-i\frac{G_F}{2}f_{B_s}f_\pi f^u_{\eta^{(\prime)}}\Big\{V_{ub}V_{us}^*[b_1(\pi^0,\eta^{(\prime)})+b_1(\eta^{(\prime)},\pi^0)]+(V_{ub}V_{us}^*+V_{cb}V_{cs}^*)\times\Big[\frac{3}{2}b_4^{ew}(\pi^0,\eta^{(\prime)})+\frac{3}{2}b_4^{ew}(\eta^{(\prime)},\pi^0)\Big]\Big\},\tag{C5}$$

$$\mathcal{A}^a(\bar{B}_s^0\to\eta^{(\prime)}\eta^{(\prime)})=-i\sqrt{2}G_Ff_{B_s}\Big\{f^u_{\eta^{(\prime)}}f^u_{\eta^{(\prime)}}\Big[V_{ub}V_{us}^*b_1(\eta^{(\prime)},\eta^{(\prime)})+(V_{ub}V_{us}^*+V_{cb}V_{cs}^*)\Big(2b_4(\eta^{(\prime)},\eta^{(\prime)})+\frac{1}{2}b_4^{ew}(\eta^{(\prime)},\eta^{(\prime)})\Big)\Big]+f^s_{\eta^{(\prime)}}f^s_{\eta^{(\prime)}}(V_{ub}V_{us}^*+V_{cb}V_{cs}^*)\Big[b_3(\eta^{(\prime)},\eta^{(\prime)})+b_4(\eta^{(\prime)},\eta^{(\prime)})-\frac{1}{2}b_3^{ew}(\eta^{(\prime)},\eta^{(\prime)})-\frac{1}{2}b_4^{ew}(\eta^{(\prime)},\eta^{(\prime)})\Big]\Big\},\tag{C6}$$

$$\mathcal{A}^a(\bar{B}_s^0\to\eta\eta')=-i\frac{G_F}{\sqrt{2}}f_{B_s}f^u_\eta f^u_{\eta'}\Big\{V_{ub}V_{us}^*[b_1(\eta',\eta)+b_1(\eta,\eta')]+(V_{ub}V_{us}^*+V_{cb}V_{cs}^*)\Big[2b_4(\eta',\eta)+2b_4(\eta,\eta')+\frac{1}{2}b_4^{ew}(\eta',\eta)+\frac{1}{2}b_4^{ew}(\eta,\eta')\Big]\Big\}-i\frac{G_F}{\sqrt{2}}f_{B_s}f^s_\eta f^s_{\eta'}(V_{ub}V_{us}^*+V_{cb}V_{cs}^*)\times\Big\{b_3(\eta',\eta)+b_3(\eta,\eta')+b_4(\eta',\eta)+b_4(\eta,\eta')-\frac{1}{2}b_3^{ew}(\eta',\eta)-\frac{1}{2}b_3^{ew}(\eta,\eta')-\frac{1}{2}b_4^{ew}(\eta',\eta)-\frac{1}{2}b_4^{ew}(\eta,\eta')\Big\},\tag{C7}$$

$$\mathcal{A}^a(\bar{B}_s^0\to\pi^-K^+)=-i\frac{G_F}{\sqrt{2}}f_{B_s}f_\pi f_K(V_{ub}V_{ud}^*+V_{cb}V_{cd}^*)\Big\{b_3(\pi^-,K^+)-\frac{1}{2}b_3^{ew}(\pi^-,K^+)\Big\},\tag{C8}$$

$$\mathcal{A}^a(\bar{B}_s^0\to K^-K^+)=-i\frac{G_F}{\sqrt{2}}f_{B_s}f_K^2\Big\{V_{ub}V_{us}^*b_1(K^+,K^-)+(V_{ub}V_{us}^*+V_{cb}V_{cs}^*)\Big[b_3(K^-,K^+)+b_4(K^+,K^-)+b_4(K^-,K^+)-\frac{1}{2}b_3^{ew}(K^-,K^+)+b_4^{ew}(K^+,K^-)-\frac{1}{2}b_4^{ew}(K^-,K^+)\Big]\Big\},\tag{C9}$$

$$\mathcal{A}^a(\bar{B}_s^0\to\pi^-\pi^+)=-i\frac{G_F}{\sqrt{2}}f_{B_s}f_\pi^2\Big\{V_{ub}V_{us}^*b_1(\pi^+,\pi^-)+(V_{ub}V_{us}^*+V_{cb}V_{cs}^*)\Big[b_4(\pi^+,\pi^-)+b_4(\pi^-,\pi^+)+b_4^{ew}(\pi^+,\pi^-)-\frac{1}{2}b_4^{ew}(\pi^-,\pi^+)\Big]\Big\}.\tag{C10}$$

APPENDIX D: THE WEAK ANNIHILATION AMPLITUDES FOR $\bar{B}_s^0\to PV$

$$\mathcal{A}^a(\bar{B}_s^0\to K^0\rho^0)=-\frac{G_F}{2}f_{B_s}f_Kf_\rho(V_{ub}V_{ud}^*+V_{cb}V_{cd}^*)\Big\{b_3(\rho^0,K^0)-\frac{1}{2}b_3^{ew}(\rho^0,K^0)\Big\},\tag{D1}$$

$$\mathcal{A}^a(\bar{B}_s^0 \to K^0\omega) = \frac{G_F}{2} f_{B_s} f_K f_\omega (V_{ub}V_{ud}^* + V_{cb}V_{cd}^*)\left\{ b_3(\omega, K^0) - \frac{1}{2} b_3^{ew}(\omega, K^0)\right\}, \tag{D2}$$

$$\mathcal{A}^a(\bar{B}_s^0 \to K^0\phi) = \frac{G_F}{\sqrt{2}} f_{B_s} f_K f_\phi (V_{ub}V_{ud}^* + V_{cb}V_{cd}^*)\left\{ b_3(K^0, \phi) - \frac{1}{2} b_3^{ew}(K^0, \phi)\right\}, \tag{D3}$$

$$\begin{aligned}\mathcal{A}^a(\bar{B}_s^0 \to K^0\bar{K}^{*0}) = \frac{G_F}{\sqrt{2}} f_{B_s} f_K f_{K^*} (V_{ub}V_{us}^* + V_{cb}V_{cs}^*)\Big\{ & b_3(\bar{K}^{*0}, K^0) + b_4(K^0, \bar{K}^{*0}) + b_4(\bar{K}^{*0}, K^0) \\ & - \frac{1}{2} b_3^{ew}(\bar{K}^{*0}, K^0) - \frac{1}{2} b_4^{ew}(K^0, \bar{K}^{*0}) - \frac{1}{2} b_4^{ew}(\bar{K}^{*0}, K^0)\Big\},\end{aligned} \tag{D4}$$

$$\begin{aligned}\mathcal{A}^a(\bar{B}_s^0 \to \bar{K}^0 K^{*0}) = \frac{G_F}{\sqrt{2}} f_{B_s} f_K f_{K^*} (V_{ub}V_{us}^* + V_{cb}V_{cs}^*)\Big\{ & b_3(\bar{K}^0, K^{*0}) + b_4(K^{*0}, \bar{K}^0) + b_4(\bar{K}^0, K^{*0}) \\ & - \frac{1}{2} b_3^{ew}(\bar{K}^0, K^{*0}) - \frac{1}{2} b_4^{ew}(K^{*0}, \bar{K}^0) - \frac{1}{2} b_4^{ew}(\bar{K}^0, K^{*0})\Big\},\end{aligned} \tag{D5}$$

$$\mathcal{A}^a(\bar{B}_s^0 \to \pi^0 K^{*0}) = -\frac{G_F}{2} f_{B_s} f_\pi f_{K^*} (V_{ub}V_{ud}^* + V_{cb}V_{cd}^*)\left\{ b_3(\pi^0, K^{*0}) - \frac{1}{2} b_3^{ew}(\pi^0, K^{*0})\right\}, \tag{D6}$$

$$\begin{aligned}\mathcal{A}^a(\bar{B}_s^0 \to \pi^0\rho^0) = \frac{G_F}{2\sqrt{2}} f_{B_s} f_\pi f_\rho \Big\{ & V_{ub}V_{us}^*[b_1(\pi^0, \rho^0) + b_1(\rho^0, \pi^0)] + (V_{ub}V_{us}^* + V_{cb}V_{cs}^*) \\ & \times\left[2b_4(\pi^0, \rho^0) + 2b_4(\rho^0, \pi^0) + \frac{1}{2} b_4^{ew}(\pi^0, \rho^0) + \frac{1}{2} b_4^{ew}(\rho^0, \pi^0)\right]\Big\},\end{aligned} \tag{D7}$$

$$\begin{aligned}\mathcal{A}^a(\bar{B}_s^0 \to \pi^0\omega) = \frac{G_F}{2\sqrt{2}} f_{B_s} f_\pi f_\omega \Big\{ & V_{ub}V_{us}^*[b_1(\pi^0, \omega) + b_1(\omega, \pi^0)] + (V_{ub}V_{us}^* + V_{cb}V_{cs}^*) \\ & \times\left[\frac{3}{2} b_4^{ew}(\pi^0, \omega) + \frac{3}{2} b_4^{ew}(\omega, \pi^0)\right]\Big\},\end{aligned} \tag{D8}$$

$$\mathcal{A}^a(\bar{B}_s^0 \to \pi^0\phi) = 0, \tag{D9}$$

$$\begin{aligned}\mathcal{A}^a(\bar{B}_s^0 \to \eta^{(\prime)} K^{*0}) = \frac{G_F}{\sqrt{2}} f_{B_s} f_{K^*} (V_{ub}V_{ud}^* + V_{cb}V_{cd}^*)\Big\{ & f_{\eta^{(\prime)}}^u\left[b_3(\eta^{(\prime)}, K^{*0}) - \frac{1}{2} b_3^{ew}(\eta^{(\prime)}, K^{*0})\right] \\ & + f_{\eta^{(\prime)}}^s\left[b_3(K^{*0}, \eta^{(\prime)}) - \frac{1}{2} b_3^{ew}(K^{*0}, \eta^{(\prime)})\right]\Big\},\end{aligned} \tag{D10}$$

$$\begin{aligned}\mathcal{A}^a(\bar{B}_s^0 \to \eta^{(\prime)}\phi) = \frac{G_F}{\sqrt{2}} f_{B_s} f_\phi f_{\eta^{(\prime)}}^s (V_{ub}V_{us}^* + V_{cb}V_{cs}^*)\Big\{ & b_3(\eta^{(\prime)}, \phi) + b_3(\phi, \eta^{(\prime)}) + b_4(\eta^{(\prime)}, \phi) + b_4(\phi, \eta^{(\prime)}) \\ & - \frac{1}{2} b_3^{ew}(\eta^{(\prime)}, \phi) - \frac{1}{2} b_3^{ew}(\phi, \eta^{(\prime)}) - \frac{1}{2} b_4^{ew}(\eta^{(\prime)}, \phi) - \frac{1}{2} b_4^{ew}(\phi, \eta^{(\prime)})\Big\},\end{aligned} \tag{D11}$$

$$\begin{aligned}\mathcal{A}^a(\bar{B}_s^0 \to \eta^{(\prime)}\rho^0) = \frac{G_F}{2} f_{B_s} f_\rho f_{\eta^{(\prime)}}^u \Big\{ & V_{ub}V_{us}^*[b_1(\eta^{(\prime)}, \rho^0) + b_1(\rho^0, \eta^{(\prime)})] + (V_{ub}V_{us}^* + V_{cb}V_{cs}^*)\left[\frac{3}{2} b_4^{ew}(\eta^{(\prime)}, \rho^0)\right. \\ & \left. + \frac{3}{2} b_4^{ew}(\rho^0, \eta^{(\prime)})\right]\Big\},\end{aligned} \tag{D12}$$

$$\mathcal{A}^a(\bar{B}_s^0 \to \eta^{(\prime)}\omega) = \frac{G_F}{2} f_{B_s} f_\omega f^u_{\eta^{(\prime)}} \Big\{ V_{ub}V^*_{us}[b_1(\eta^{(\prime)},\omega) + b_1(\omega,\eta^{(\prime)})] + (V_{ub}V^*_{us} + V_{cb}V^*_{cs}) \times \Big[2b_4(\eta^{(\prime)},\omega) + 2b_4(\omega,\eta^{(\prime)}) + \frac{1}{2} b_4^{ew}(\eta^{(\prime)},\omega) + \frac{1}{2} b_4^{ew}(\omega,\eta^{(\prime)}) \Big] \Big\}, \tag{D13}$$

$$\mathcal{A}^a(\bar{B}_s^0 \to K^+\rho^-) = \frac{G_F}{\sqrt{2}} f_{B_s} f_\rho f_K (V_{ub}V^*_{ud} + V_{cb}V^*_{cd}) \Big\{ b_3(\rho^-,K^+) - \frac{1}{2} b_3^{ew}(\rho^-,K^+) \Big\}, \tag{D14}$$

$$\mathcal{A}^a(\bar{B}_s^0 \to K^+K^{*-}) = \frac{G_F}{\sqrt{2}} f_{B_s} f_K f_{K^*} \Big\{ V_{ub}V^*_{us} b_1(K^+,K^{*-}) + (V_{ub}V^*_{us} + V_{cb}V^*_{cs}) \times \Big[b_3(K^{*-},K^+) + b_4(K^+,K^{*-}) + b_4(K^{*-},K^+) - \frac{1}{2} b_3^{ew}(K^{*-},K^+) + b_4^{ew}(K^+,K^{*-}) - \frac{1}{2} b_4^{ew}(K^{*-},K^+) \Big] \Big\}, \tag{D15}$$

$$\mathcal{A}^a(\bar{B}_s^0 \to K^-K^{*+}) = \frac{G_F}{\sqrt{2}} f_{B_s} f_K f_{K^*} \Big\{ V_{ub}V^*_{us} b_1(K^{*+},K^-) + (V_{ub}V^*_{us} + V_{cb}V^*_{cs}) \Big[b_3(K^-,K^{*+}) + b_4(K^{*+},K^-) + b_4(K^-,K^{*+}) - \frac{1}{2} b_3^{ew}(K^-,K^{*+}) + b_4^{ew}(K^{*+},K^-) - \frac{1}{2} b_4^{ew}(K^-,K^{*+}) \Big] \Big\}, \tag{D16}$$

$$\mathcal{A}^a(\bar{B}_s^0 \to \pi^+\rho^-) = \frac{G_F}{\sqrt{2}} f_{B_s} f_\pi f_\rho \Big\{ V_{ub}V^*_{us} b_1(\pi^+,\rho^-) + (V_{ub}V^*_{us} + V_{cb}V^*_{cs}) \Big[b_4(\pi^+,\rho^-) + b_4(\rho^-,\pi^+) + b_4^{ew}(\pi^+,\rho^-) - \frac{1}{2} b_4^{ew}(\rho^-,\pi^+) \Big] \Big\}, \tag{D17}$$

$$\mathcal{A}^a(\bar{B}_s^0 \to \pi^-\rho^+) = \frac{G_F}{\sqrt{2}} f_{B_s} f_\pi f_\rho \Big\{ V_{ub}V^*_{us} b_1(\rho^+,\pi^-) + (V_{ub}V^*_{us} + V_{cb}V^*_{cs}) \Big[b_4(\rho^+,\pi^-) + b_4(\pi^-,\rho^+) + b_4^{ew}(\rho^+,\pi^-) - \frac{1}{2} b_4^{ew}(\pi^-,\rho^+) \Big] \Big\}, \tag{D18}$$

$$\mathcal{A}^a(\bar{B}_s^0 \to \pi^-K^{*+}) = \frac{G_F}{\sqrt{2}} f_{B_s} f_\pi f_{K^*} (V_{ub}V^*_{ud} + V_{cb}V^*_{cd}) \Big\{ b_3(\pi^-,K^{*+}) - \frac{1}{2} b_3^{ew}(\pi^-,K^{*+}) \Big\}. \tag{D19}$$

[1] D.G. Cassel, Int. J. Mod. Phys. A **17**, 2951 (2002).
[2] BABAR Collaboration, S. Willocq, Nucl. Phys. B (Proc. Suppl.) **111**, 34 (2002).
[3] BABAR Collaboration, B. Aubert *et al.*, hep-ex/0206053.
[4] BABAR Collaboration, B. Aubert *et al.*, Phys. Rev. Lett. **89**, 281802 (2002).
[5] BABAR Collaboration, B. Aubert *et al.*, hep-ex/0207065.
[6] Belle Collaboration, H. Tajima, Int. J. Mod. Phys. A **17**, 2967 (2002).
[7] Belle Collaboration, K. Abe *et al.*, Phys. Rev. Lett. **89**, 071801 (2002); Phys. Rev. D **68**, 012001 (2003).
[8] Belle Collaboration, A. Gordon *et al.*, Phys. Lett. B **542**, 183 (2002).
[9] Belle Collaboration, K.F. Chen *et al.*, Phys. Lett. B **546**, 196 (2002).
[10] Belle Collaboration, B.C.K. Casey *et al.*, Phys. Rev. D **66**, 092002 (2002).
[11] M. Beneke, G. Buchalla, M. Neubert, and C.T. Sachrajda, Phys. Rev. Lett. **83**, 1914 (1999); Nucl. Phys. **B591**, 313 (2000).
[12] C.H. Chang and H.N. Li, Phys. Rev. D **55**, 5577 (1997).
[13] T.W. Yeh and H.N. Li, Phys. Rev. D **56**, 1615 (1997).

[14] Y.Y. Keum, H.N. Li, and A.I. Sanda, Phys. Lett. B **504**, 6 (2001); Phys. Rev. D **63**, 054008 (2001).
[15] A. Ali, G. Kramer, and C.D. Lü, Phys. Rev. D **58**, 094009 (1998); **59**, 014005 (1999).
[16] Y.H. Chen, H.Y. Cheng, B. Tseng, and K.C. Yang, Phys. Rev. D **60**, 094014 (1999).
[17] M.Z. Yang and Y.D. Yang, Nucl. Phys. **B609**, 469 (2001).
[18] H.Y. Cheng and K.C. Yang, Phys. Lett. B **511**, 40 (2001); Phys. Rev. D **62**, 054029 (2000).
[19] D.S. Du, D.S. Yang, and G.H. Zhu, Phys. Lett. B **488**, 46 (2000).
[20] M. Beneke, G. Buchalla, M. Neubert, and C.T. Sachrajda, Nucl. Phys. **B606**, 245 (2001).
[21] D.S. Du, H.J. Gong, J.F. Sun, D.S. Yang, and G.H. Zhu, Phys. Rev. D **65**, 074001 (2002).
[22] D.S. Du, H.J. Gong, J.F. Sun, D.S. Yang, and G.H. Zhu, Phys. Rev. D **65**, 094025 (2002); **66**, 079904(E) (2002).
[23] N. Cabibbo, Phys. Rev. Lett. **10**, 351 (1963); M. Kobayashi and T. Maskawa, Prog. Theor. Phys. **49**, 652 (1973).
[24] Particle Data Group, K. Hagiwara *et al.*, Phys. Rev. D **66**, 010001 (2002) (http://pdg.lbl.gov).
[25] D. Du and Zi Wang, Phys. Rev. D **38**, 3570 (1988).
[26] A. Deandrea, N. Di Bartolomeo, R. Gatto, and G. Nardulli, Phys. Lett. B **318**, 549 (1993).
[27] A. Deandrea *et al.*, Phys. Lett. B **320**, 170 (1993).
[28] D.S. Du and Z.Z. Xing, Phys. Rev. D **48**, 3400 (1993).
[29] D.S. Du and M.Z. Yang, Phys. Lett. B **358**, 123 (1995).
[30] B. Tseng, Phys. Lett. B **446**, 125 (1999).
[31] Y.H. Chen, H.Y. Cheng, and B. Tseng, Phys. Rev. D **59**, 074003 (1999).
[32] D. Zhang, Z.J. Xiao, and C.S. Li, Phys. Rev. D **64**, 014014 (2001).
[33] D.S. Du, D.S. Yang, and G.H. Zhu, Phys. Lett. B **509**, 263 (2001); Phys. Rev. D **64**, 014036 (2001).
[34] D.S. Du, J.F. Sun, D.S. Yang, and G.H. Zhu, Phys. Rev. D **67**, 014023 (2003).
[35] For a review, see G. Buchalla, A.J. Buras, and M.E. Lautenbacher, Rev. Mod. Phys. **68**, 1125 (1996); or A.J. Buras, hep-ph/9806471.
[36] M. Wirbel, B. Stech, and M. Bauer, Z. Phys. C **29**, 637 (1985); M. Bauer, B. Stech, and M. Wirbel, *ibid.* **34**, 103 (1987).
[37] D.S. Du, C.S. Huang, Z.T. Wei, and M.Z. Yang, Phys. Lett. B **520**, 50 (2001).
[38] S. Descotes-Genon and C.T. Sachrajda, Nucl. Phys. **B625**, 239 (2002).
[39] Z.T. Wei and M.Z. Yang, Nucl. Phys. **B642**, 263 (2002).
[40] Y.Y. Keum and H.N. Li, Phys. Rev. D **63**, 074006 (2001).
[41] C.D. Lü, K. Ukai, and M.Z. Yang, Phys. Rev. D **63**, 074009 (2001).
[42] L. Wolfenstein, Phys. Rev. Lett. **51**, 1945 (1983).
[43] M. Ciuchini *et al.*, J. High Energy Phys. **07**, 013 (2001).
[44] A. Höcker, H. Lacker, S. Laplace, and F. Le Diberder, Eur. Phys. J. C **21**, 225 (2001); in *Heavy Flavor Physics*, edited by Anders Ryd and Frank C. Porter, AIP Conf. Proc. No. 618 (AIP, Melville, NY, 2002), p. 27. For an update, see http://www.slac.stanford.edu/~laplace/ckmfitter.html.
[45] A.J. Buras, F. Parodi, and A. Stocchi, J. High Energy Phys. **01**, 029 (2003).
[46] M. Bargiotti *et al.*, Eur. Phys. J. C **24**, 361 (2002).
[47] M. Beneke, talk presented at Flavor Physics & CP Violation (FPCP), Philadelphia, 2002, hep-ph/0207228; M. Neubert, talk presented at the International Workshop on Heavy Quarks & Leptons, Vietri sul mare, Salerno, Italy, hep-ph/0207327.
[48] T. Feldmann, P. Kroll, and B. Stech, Phys. Rev. D **58**, 114006 (1998).
[49] M. Beneke and M. Neubert, Nucl. Phys. **B651**, 225 (2003).
[50] S. Narison, Phys. Lett. B **520**, 115 (2001).
[51] R.L. Jaffe and X. Ji, Nucl. Phys. **B357**, 527 (1992); P. Ball, V.M. Braun, Y. Koike, and K. Tanaka, *ibid.* **B529**, 323 (1998).
[52] M. Beneke and Th. Feldmann, Nucl. Phys. **B592**, 3 (2001).
[53] P. Ball and V.M. Braun, Phys. Rev. D **54**, 2182 (1996).
[54] CLEO Collaboration, S.J. Richichi *et al.*, Phys. Rev. Lett. **85**, 520 (2000).
[55] D. Atwood and A. Soni, Phys. Lett. B **405**, 150 (1997).
[56] W. Hou and B. Tseng, Phys. Rev. Lett. **80**, 434 (1998).
[57] D.S. Du, C.S. Kim, and Y.D. Yang, Phys. Lett. B **426**, 133 (1998).
[58] M.R. Ahmady, E. Kou, and A. Sugamoto, Phys. Rev. D **58**, 014015 (1998).
[59] A. Ali and D. London, Z. Phys. C **65**, 431 (1995).
[60] M. Gronau and J.L. Rosner, Phys. Rev. D **65**, 113008 (2002).
[61] R. Fleischer, hep-ph/0011323.
[62] P. Ball *et al.*, hep-ph/0003238.
[63] BABAR Collaboration, B. Aubert *et al.*, Sov. Phys. JETP **74**, 216 (2001).
[64] Belle Collaboration, K. Abe *et al.*, Phys. Rev. D **66**, 032007 (2002).
[65] M. Gronau and J.L. Rosner, Phys. Rev. D **65**, 013004 (2002); **65**, 079901(E) (2002).